

# Adiabaticity and spectral splits in collective neutrino transformations

Georg G. Raffelt<sup>1</sup> and Alexei Yu. Smirnov<sup>2,3</sup>

<sup>1</sup>*Max-Planck-Institut für Physik (Werner-Heisenberg-Institut), Föhringer Ring 6, 80805 München, Germany*

<sup>2</sup>*Abdus Salam International Centre for Theoretical Physics, Strada Costiera 11, 34014 Trieste, Italy*

<sup>3</sup>*Institute for Nuclear Research, Russian Academy of Sciences,  
60th October Anniversary Prospect 7A, 117 312 Moscow, Russia*

(Dated: 28 September 2007)

Neutrinos streaming off a supernova core transform collectively by neutrino-neutrino interactions, leading to “spectral splits” where an energy  $E_{\text{split}}$  divides the transformed spectrum sharply into parts of almost pure but different flavors. We present a detailed description of the spectral split phenomenon which is conceptually and quantitatively understood in an adiabatic treatment of neutrino-neutrino effects. Central to this theory is a self-consistency condition in the form of two sum rules (integrals over the neutrino spectra that must equal certain conserved quantities). We provide explicit analytic and numerical solutions for various neutrino spectra. We introduce the concept of the adiabatic reference frame and elaborate on the relative adiabatic evolution. Violating adiabaticity leads to the spectral split being “washed out.” The sharpness of the split appears to be represented by a surprisingly universal function.

PACS numbers: 14.60.Pq, 97.60.Bw

## I. INTRODUCTION

In a dense neutrino gas, neutrino-neutrino refraction causes nonlinear flavor oscillation phenomena [1, 2, 3, 4, 5, 6, 7, 8, 9, 10, 11, 12, 13, 14, 15, 16, 17, 18]. In the region between the neutrino sphere and a radius of several hundred kilometers in a core-collapse supernova (SN), the flavor content of neutrino fluxes is dramatically modified [7, 8, 9, 10, 11, 12, 13, 14, 15, 16, 17, 18]. Ordinary MSW resonances typically occur at much larger distances and process the spectra further in well-understood ways [19, 20].

One particularly intriguing feature of the emerging fluxes is a “spectral split.” What this means is best described with the help of an example. In Fig. 1 we show thermal  $\nu_e$  and  $\bar{\nu}_e$  flux spectra with an average energy of 15 MeV produced in the neutrino sphere of a SN core (thin lines). This example is schematic in that we assume equal average  $\nu_e$  and  $\bar{\nu}_e$  energies but an overall  $\bar{\nu}_e$  flux that is only 70% of the  $\nu_e$  flux. Moreover, the smaller fluxes of the other species  $\nu_\mu$ ,  $\nu_\tau$ ,  $\bar{\nu}_\mu$  and  $\bar{\nu}_\tau$  are completely ignored. We are considering two-flavor oscillations between  $\nu_e$  and another flavor  $\nu_x$ , driven by the atmospheric mass squared difference  $\Delta m^2 = 2 - 3 \times 10^{-3} \text{ eV}^2$  and the small 1-3 mixing angle. Therefore in Fig. 1 we show the  $z$ -components of the usual two-flavor polarization vectors, where “up” denotes the electron flavor and “down” the  $x$ -flavor. In other words, the spectrum represents electron (anti)neutrinos where it is positive and  $x$  (anti)neutrinos where it is negative.

After a few 100 km, the neutrino-neutrino effects have completely died out. The emerging spectra are shown as thick lines. The antineutrinos (dashed) have completely flipped to the  $x$ -flavor. The same is true for the neutrinos (solid) down to a critical energy  $E_{\text{split}}$  where the spectrum splits. All  $\nu_e$  below this energy emerge in their original flavor. Spectral splits of this sort were first ob-

served in the numerical simulations of Duan et al. [9] where a first interpretation was given. Later these authors have introduced the term “stepwise spectral swapping” to describe this phenomenon [17].

In a previous short paper [14] we have shown that  $E_{\text{split}}$  is fixed by what we call lepton-number conservation. For a sufficiently small in-medium mixing angle the collective flavor transformations have the property of conserving flavor number in the sense that only pairs  $\nu_e \bar{\nu}_e$  are transformed to pairs  $\nu_x \bar{\nu}_x$ , whereas the excess  $\nu_e$  flux is conserved [11]. While this property does not explain the existence of a spectral split, it explains its location that for the example of Fig. 1 is at  $E_{\text{split}} = 9.57 \text{ MeV}$ .

The split phenomenon becomes clearer when the spectra are represented in terms of the oscillation frequency

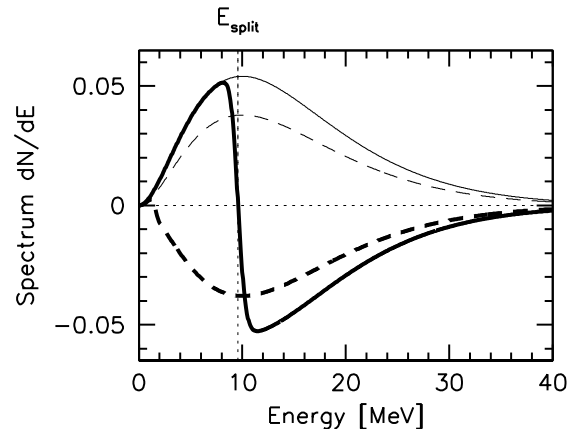


FIG. 1: Neutrino spectra at the neutrino sphere (thin lines) and beyond the dense-neutrino region (thick lines) for the schematic SN model described in the text. Solid: neutrinos. Dashed: antineutrinos. Positive spectrum: electron (anti)neutrinos. Negative spectrum:  $x$  (anti)neutrinos.

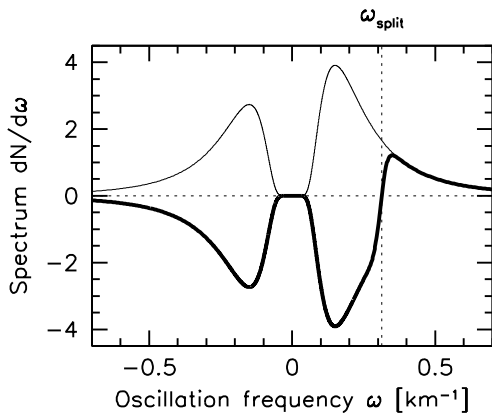


FIG. 2: Same as Fig. 1, now with  $\omega = \Delta m^2/2E$  as independent variable:  $\omega < 0$  is for antineutrinos,  $\omega > 0$  for neutrinos.

$\omega \equiv \Delta m^2/2E$  instead of the energy itself [14]. In the evolution equations the only difference between neutrinos and antineutrinos is that the latter appear with a negative  $\omega$ . Therefore, one should think of the neutrino and antineutrino spectra as a single continuum  $-\infty < \omega < +\infty$ . The two spectra merge at the point  $\omega = 0$  that represents both a neutrino or antineutrino of infinite energy. In Fig. 2 we show the example of Fig. 1 in terms of the  $\omega$ -variable where  $\omega_{\text{split}} = 0.314 \text{ km}^{-1}$ . All modes with  $\omega < \omega_{\text{split}}$  are transformed whereas the ones with  $\omega > \omega_{\text{split}}$  stay in their original flavor.

The split occurs among the neutrinos ( $\omega_{\text{split}} > 0$ ) because a SN core deleptonizes, producing an excess  $\nu_e$  flux. On the other hand, an excess of the  $\bar{\nu}_e$ -flux is typical for the leptonizing accretion torus of merging neutron stars that are probably the central engines of short gamma-ray bursts. Here we have  $\omega_{\text{split}} < 0$  and the situation is reversed: All modes with  $\omega > \omega_{\text{split}}$  convert (Sec. III C). However, we will always use an excess  $\nu_e$  flux without loss of generality.

The interpretation of the split phenomenon proposed by Duan et al. [12] motivated us to develop a quantitative theory of this effect based on the idea of adiabatic evolution of individual modes [14]. While the self-interacting neutrino ensemble follows a set of nonlinear equations of motion (EOMs), the evolution of individual modes can be written in the form of single-particle EOMs where the neutrino-neutrino interaction is included self-consistently by a slowly varying “mean field” in the single-mode Hamiltonians. The crucial step was to obtain two sum rules (integrals over the neutrino spectrum in the  $\omega$ -variable) that had to equal certain conserved quantities, notably the flavor lepton number of the system [14]. These sum rules provide an explicit adiabatic solution of the problem.

The degree of adiabaticity manifests itself in the “sharpness” of the spectral split. The adiabatic evolution is driven by the decreasing neutrino-neutrino interaction strength as a function of distance from the SN core. As we dial the scale height to larger values, the spectral split

becomes sharper, approaching a step function in the limit of an infinitely slow evolution.

This situation is similar to the usual MSW case, for example in the outer layers of a SN envelope. The  $\nu_e$  flux streaming through a resonance region completely converts, for the normal hierarchy, while the antineutrinos remain unchanged. In other words, in the case of perfect adiabaticity the usual MSW effect is a spectral-split phenomenon with  $\omega_{\text{split}} = 0$ . In this sense the main effect of the neutrino-neutrino interaction is to shift  $\omega_{\text{split}}$  to a non-vanishing value. We will further discuss this analogy in the context of adiabaticity breaking in Sec. VII.

The main purpose of our paper is to elaborate several issues that were kept short in our previous publication [14]. In addition, we will pay greater attention to the actual definition of what we mean with adiabaticity and we will study phenomena caused by deviations from a purely adiabatic evolution. We begin in Sec. II with a description of the framework for our study: the EOMs and our simplifications and approximations. In Sec. III we present the adiabatic solution in the form of two sum rules. The following Secs. IV–VI are dedicated to explicit analytic and numerical solutions of the EOMs in particular cases. In Sec. VII we study the impact of deviations from perfect adiabaticity. We conclude in Sec. VIII.

## II. FRAMEWORK AND SIMPLIFICATIONS

### A. Equations of motion (EOMs)

Nonlinear flavor transformations caused by neutrino-neutrino interactions involve two main complications. One is the energy dependence of the effect, a question that we will address here. The other is the “multi-angle” nature of the transformations. If a neutrino gas is not perfectly isotropic, neutrinos moving in different directions feel a different refractive effect caused by the other neutrinos because the interaction energy between two neutrinos depends on their relative direction as  $(1 - \cos \theta)$ . As a consequence, one expects kinematical decoherence of the flavor content of different angular modes. For equal densities of neutrinos and antineutrinos, decoherence indeed occurs and is even self-accelerating in that an infinitesimally small anisotropy is enough to trigger an exponential runaway towards complete flavor equilibrium [13]. On the other hand, if the neutrino-neutrino interaction decreases slowly and if the asymmetry between  $\nu_e$  and  $\bar{\nu}_e$  is sufficiently large, one observes numerically that decoherence is suppressed. In the SN context, the deleptonization flux appears to be large enough to prevent multi-angle decoherence [15].

Therefore, we limit ourselves to an isotropic gas with a slowly decreasing density. The ensemble is fully characterized by a matrix of densities in flavor space for each spectral component  $E$ , separately for neutrinos and antineutrinos. The energies enter only through the vacuum oscillation frequencies  $\omega \equiv \Delta m^2/2E$  which determine the

behavior of different modes. Therefore, it is more convenient to use  $\omega$  directly to label the modes. In the two-flavor context we use the usual polarization vectors so that the ensemble is represented by two sets of polarization vectors  $\mathbf{P}_\omega$  and  $\bar{\mathbf{P}}_\omega$ . The global polarization vectors,

$$\mathbf{P} = \int_0^\infty d\omega \mathbf{P}_\omega \quad \text{and} \quad \bar{\mathbf{P}} = \int_0^\infty d\omega \bar{\mathbf{P}}_\omega, \quad (1)$$

are initially normalized as

$$P = |\mathbf{P}| = 1 \quad \text{and} \quad \bar{P} = |\bar{\mathbf{P}}| = \alpha < 1. \quad (2)$$

Notice that  $\mathbf{P}_\omega$  and  $\bar{\mathbf{P}}_\omega$  are densities relative to the  $\omega$  variable so that they have the dimension of  $\omega^{-1}$ . The individual lengths  $P_\omega = |\mathbf{P}_\omega|$  and  $\bar{P}_\omega = |\bar{\mathbf{P}}_\omega|$  are conserved as long as oscillations are the only form of evolution, i.e., in the absence of dynamical decoherence caused by collisions. In contrast, the total lengths  $P$  and  $\bar{P}$  are only conserved when all individual polarization vectors evolve in the same way.  $P_\omega$  and  $\bar{P}_\omega$  are the spectra of frequencies given by an initial condition.

We assume that initially all  $\mathbf{P}_\omega$  and  $\bar{\mathbf{P}}_\omega$  are aligned. In other words, all neutrinos and antineutrinos begin in the electron flavor. It is straightforward to generalize this assumption to a situation where some modes begin in the  $x$ -flavor (“spectral cross-over,” see Sec. IV C). In this more general case, the  $\mathbf{P}_\omega$  and  $\bar{\mathbf{P}}_\omega$  may initially also be anti-aligned relative to the common flavor direction.

Following the notation of Ref. [11] let us introduce the difference vector

$$\mathbf{D} \equiv \mathbf{P} - \bar{\mathbf{P}}, \quad (3)$$

representing the net lepton number. Using the conventions of Ref. [21], the EOMs are

$$\begin{aligned} \partial_t \mathbf{P}_\omega &= (+\omega \mathbf{B} + \lambda \mathbf{L} + \mu \mathbf{D}) \times \mathbf{P}_\omega, \\ \partial_t \bar{\mathbf{P}}_\omega &= (-\omega \mathbf{B} + \lambda \mathbf{L} + \mu \mathbf{D}) \times \bar{\mathbf{P}}_\omega, \end{aligned} \quad (4)$$

where  $\mathbf{B} = (\sin 2\theta, 0, \cos 2\theta)$  is the mass direction and  $\theta$  the vacuum mixing angle. For the inverted mass hierarchy  $\theta \sim \pi/2$ . The unit vector  $\mathbf{L} = (0, 0, 1)$  is the weak charged-current interaction direction so that  $\mathbf{B} \cdot \mathbf{L} = \cos 2\theta$ . Finally,  $\lambda \equiv \sqrt{2}G_F n_e$  is the usual matter potential and  $\mu \equiv \sqrt{2}G_F n_\nu$  the potential due to neutrino-neutrino interactions with  $n_e$  and  $n_\nu$  being the electron and neutrino densities. We use time  $t$  instead of radius  $r$  because we study an isotropic system that evolves in time instead of a single-angle system evolving in space.

In the SN context, the neutrino flux dilutes as  $r^{-2}$ . Moreover, the trajectories become more collinear with distance, leading to an average suppression of the interaction energy by another factor  $r^{-2}$  [4] so that altogether we should use  $\mu(t) \propto t^{-4}$ . However, in the adiabatic limit the exact form of  $\mu(t)$  is irrelevant as long as its rate of change is small. For our numerical examples it is more convenient to use the profile

$$\mu(t) = \mu_0 \exp(-t/\tau). \quad (5)$$

The exponential form is simpler because it involves the same scale  $|d \ln \mu(t)/dt|^{-1} = \tau$  at all times. Adjusting  $\tau$  allows one to control the adiabaticity of the transition with a single parameter. Assuming the atmospheric  $\Delta m^2$  and typical SN neutrino energies, we find that  $\omega_0 = 0.3 \text{ km}^{-1}$  is typical for the average vacuum oscillation frequency. The crucial action takes place at the relatively large radius of a few hundred kilometers. Together with the  $r^{-4}$  scaling this implies a characteristic rate of change of  $0.01 \text{ km}^{-1}$ . Therefore, in Eq. (5) a value  $\tau = (0.03 \omega_0)^{-1}$  roughly captures the situation in a SN.

## B. Removing the usual matter effect

Unless there is an MSW resonance in the dense-neutrino region, one can eliminate  $\lambda \mathbf{L}$  from Eq. (4) by going into a rotating frame [8, 11]. The price for this transformation is that in the new frame  $\mathbf{B}$  has a static component  $B_L = B \cos 2\theta$  along the  $\mathbf{L}$  direction and a fast-rotating one in the transverse direction. Assuming that the effect of the fast-rotating component averages to zero, we may consider the equivalent situation where the usual matter is completely absent and initially all polarization vectors are aligned with  $\mathbf{B}$  (which really is the projection of the true  $\mathbf{B}$  on the weak-interaction direction  $\mathbf{L}$ ). This is equivalent to a vanishing vacuum mixing angle.

Of course, this is not the complete story because for a strictly vanishing vacuum mixing angle, no transformation effects would take place at all. The rotating component of  $\mathbf{B}$  disturbs the perfect alignment of  $\mathbf{P}_\omega$  and  $\bar{\mathbf{P}}_\omega$ , providing a kick start for flavor conversions [8]. For a system consisting of equal numbers of neutrinos and antineutrinos, the equations were solved analytically [11]. The net effect was found to be equivalent to a small (but nonvanishing) effective mixing angle, although the evolution of the polarization vectors is initially modulated by the rotating  $\mathbf{B}$  field with the frequency  $\lambda$ . We have here a different system where the density of neutrinos exceeds that of antineutrinos and where the evolution of the system is driven by the  $\mu(t)$  variation. Numerically one finds that once more the effect of matter is equivalent to reducing the vacuum mixing angle to a certain effective mixing angle  $\theta_{\text{eff}}$  similar to the usual in-medium mixing angle [15], but an analytic treatment of how ordinary matter modifies the initial evolution is not available.

Motivated by this evidence we make the simplification of ignoring the ordinary matter term entirely, schematically accounting for it by a small initial effective mixing angle. Notice that in the absence of the interaction vector  $\mathbf{L}$  we define the effective mixing angle as the angle between  $\mathbf{D}$  and  $\mathbf{B}$ . Our treatment is exact for a system where the only interaction is that of the neutrinos among each other. While we cannot claim with mathematical rigor that this system is a faithful proxy for what happens in a real SN, numerical observations suggest that this is the case.

### C. EOMs in the $\omega$ variable

The equation of motion for  $\bar{\mathbf{P}}_\omega$  differs from that for  $\mathbf{P}_\omega$  only by the sign of frequency:  $\omega \rightarrow -\omega$ . So, the only difference for antineutrinos is that in vacuum they oscillate “the other way round.” Therefore, instead of using  $\bar{\mathbf{P}}_\omega$  we may extend  $\mathbf{P}_\omega$  to negative frequencies such that  $\bar{\mathbf{P}}_\omega = \mathbf{P}_{-\omega}$  ( $\omega > 0$ ) and use only  $\mathbf{P}_\omega$  with  $-\infty < \omega < +\infty$ . After eliminating the matter term  $\lambda \mathbf{L}$  the EOMs then take on the simple form

$$\dot{\mathbf{P}}_\omega = (\omega \mathbf{B} + \mu \mathbf{D}) \times \mathbf{P}_\omega. \quad (6)$$

A compact expression for the difference vector is

$$\mathbf{D} = \int_{-\infty}^{+\infty} d\omega s_\omega \mathbf{P}_\omega, \quad (7)$$

where

$$s_\omega \equiv \text{sign}(\omega) = \frac{\omega}{|\omega|}. \quad (8)$$

Integrating both sides of Eq. (6) over  $s_\omega d\omega$  provides

$$\dot{\mathbf{D}} = \mathbf{B} \times \mathbf{M}, \quad (9)$$

where

$$\mathbf{M} \equiv \int_{-\infty}^{+\infty} d\omega s_\omega \omega \mathbf{P}_\omega \quad (10)$$

is the “effective magnetic moment” of the system.

The EOM for  $\mathbf{D}$  is not a closed differential equation. However, when  $\mu$  is large, all  $\mathbf{P}_\omega$  ( $-\infty < \omega < \infty$ ) remain pinned to each other, and therefore  $\mathbf{M} \propto \mathbf{D}$ . In this case, according to Eq. (9) the collective vector  $\mathbf{D}$  precesses around  $\mathbf{B}$  with the synchronization frequency [6]

$$\omega_{\text{synch}} = \frac{M}{D} = \frac{\int_{-\infty}^{+\infty} d\omega s_\omega \omega P_\omega}{\int_{-\infty}^{+\infty} d\omega P_\omega}. \quad (11)$$

If  $\mu$  is suddenly turned off, all  $\mathbf{P}_\omega$  henceforth precess with their individual  $\omega$ . The transverse component of  $\mathbf{D}$  quickly averages to zero (kinematical decoherence), whereas the component along  $\mathbf{B}$  is conserved. We will here study the opposite limit where  $\mu$  decreases slowly, leading to a very different final result.

### D. Lepton-number conservation

Since  $\mathbf{B}$  is constant, Eq. (9) shows that  $\partial_t(\mathbf{D} \cdot \mathbf{B}) = 0$  and therefore

$$D_{\parallel} = \mathbf{B} \cdot \mathbf{D} = \text{const.}, \quad (12)$$

where here and henceforth we will denote the component of a vector parallel to  $\mathbf{B}$  with the index  $\parallel$ , the transverse component with the index  $\perp$ .

The physical interpretation of the conservation law Eq. (12) is what we call “flavor lepton-number conservation” or simply “lepton-number conservation.” Rigorously it only means that in the absence of matter the projection of  $\mathbf{D}$  on  $\mathbf{B}$  is conserved. However, in all examples of practical interest in the SN context, the effective mixing angle is small so that initially  $\mathbf{D}$  and  $\mathbf{B}$  are nearly collinear. Therefore, the net  $\nu_e$  flux from deleptonization is approximately conserved until an MSW resonance is encountered. Collective effects only induce pair transformations of the form  $\nu_e \bar{\nu}_e \rightarrow \nu_x \bar{\nu}_x$ , whereas the excess of the  $\nu_e$  flux from deleptonization is conserved.

## III. ADIABATIC SOLUTION

### A. Adiabaticity and co-rotating plane

To understand the evolution of our system in the limit of a slowly changing  $\mu$ , we rewrite the EOMs as

$$\dot{\mathbf{P}}_\omega = \mathbf{H}_\omega \times \mathbf{P}_\omega, \quad (13)$$

where  $-\infty < \omega < +\infty$ . We have introduced an “individual Hamiltonian” for each mode

$$\mathbf{H}_\omega = \omega \mathbf{B} + \mu \mathbf{D}. \quad (14)$$

According to the standard notion, the evolution is adiabatic when the rate of change  $\omega^{\text{eff}}(\mathbf{H}_\omega)$  of each  $\mathbf{H}_\omega$  is slow compared to the precession speed  $\omega^{\text{eff}}(\mathbf{P}_\omega)$  of  $\mathbf{P}_\omega$ :

$$\omega^{\text{eff}}(\mathbf{P}_\omega) \gg \omega^{\text{eff}}(\mathbf{H}_\omega). \quad (15)$$

In this case  $\mathbf{P}_\omega$  follows  $\mathbf{H}_\omega$ . In general  $\mathbf{P}_\omega$  need not coincide with  $\mathbf{H}_\omega$  but rather moves around  $\mathbf{H}_\omega$  on the surface of a cone whose axis coincides with  $\mathbf{H}_\omega$  and the cone angle is constant.

Let us check the adiabaticity condition for our system. Since  $|D| \leq 1 + \alpha$ , the speed (effective frequency) of the  $\mathbf{P}_\omega$  motion can be estimated according to Eq. (13) as

$$\omega^{\text{eff}}(\mathbf{P}_\omega) \leq \sqrt{\omega^2 + \mu^2(1 + \alpha)^2}. \quad (16)$$

$\mathbf{D}$  and therefore  $\mathbf{H}_\omega$  precess around  $\mathbf{B}$  with the synchronization frequency of Eq. (11):

$$\omega^{\text{eff}}(\mathbf{H}_\omega) = \omega_{\text{synch}} \sim \omega_0, \quad (17)$$

where  $\omega_0$  is some typical frequency in the spectrum. The Hamiltonian  $\mathbf{H}_\omega$  changes both because of the  $\mu$ -decrease and because of the precession of  $\mathbf{D}$ . For  $\mu \sim \omega_0$  or smaller we have

$$\omega^{\text{eff}}(\mathbf{P}_\omega) \sim \omega^{\text{eff}}(\mathbf{H}_\omega), \quad (18)$$

and therefore the adiabaticity condition that requires much faster motion of  $\mathbf{P}_\omega$  is not fulfilled. Apparently though the adiabaticity condition is fulfilled for  $\mu \gg \omega_0$ .

However, it is usually not stressed that the question of adiabaticity depends on the coordinate system and therefore adiabaticity has a relative meaning. For a single polarization vector the evolution is trivially adiabatic in a reference frame co-moving with its evolution, although this observation is useless as a means for solving the EOM. It is also trivial to find a frame where the evolution is non-adiabatic. Even for the case of the ordinary MSW effect we can go into a frame that rotates with a large frequency around the  $z$ -direction. In this frame the evolution does not look adiabatic. Of course, the final outcome is unchanged because the physical evolution does not depend on the coordinate system in which it is discussed, but the interpretation is different. In the fast-rotating frame the ordinary MSW effect is interpreted as a parametric resonance caused by a  $\mathbf{B}$ -field with a fast-rotating transverse component.

Let us return to the case at hand. Inspecting Eq. (14) reveals that the fast motion of the single-mode Hamiltonians in the “laboratory frame” is caused by the fast motion of the single common vector  $\mathbf{D}$ . If the motion of  $\mathbf{D}$  is essentially a precession around  $\mathbf{B}$  as suggested by Eq. (9), the relevant co-moving frame is simply the plane of  $\mathbf{B}$  and  $\mathbf{D}$  that rotates around  $\mathbf{B}$ . In other words, while both  $\mathbf{H}_\omega$  and  $\mathbf{P}_\omega$  precess fast around  $\mathbf{B}$ , in the co-rotating frame they may move slowly relative to each other and relative to the common frame which then plays the role of the adiabatic frame for all  $\mathbf{P}_\omega$ .

Going to a rotating frame to simplify the EOMs was first suggested by Duan et al. [8], but later they have questioned that the evolution can then be called adiabatic because it is not adiabatic in the laboratory frame [16]. We believe that the notion of adiabaticity is nevertheless appropriate because the laboratory frame is not special. (In fact, we have already transformed away the usual matter effect by going into a rotating frame which for us plays the role of the laboratory frame.) The evolution of the multi-mode system should be called adiabatic if there exists a common frame in which all modes evolve adiabatically.

In the present context, the co-rotating frame spanned by  $\mathbf{B}$  and  $\mathbf{D}$  naturally provides a common adiabatic frame. Independently of the motion of the individual  $\mathbf{P}_\omega$  that define the overall  $\mathbf{D}$ , the single-mode Hamiltonians  $\mathbf{H}_\omega$  always lie in a single plane spanned by the vectors  $\mathbf{B}$  and  $\mathbf{D}$ . Relative to the laboratory frame, this common or co-rotating plane moves around  $\mathbf{B}$  with the instantaneous co-rotating frequency  $\omega_c$ . The Hamiltonians in the co-rotating frame are

$$\mathbf{H}_\omega = (\omega - \omega_c) \mathbf{B} + \mu \mathbf{D}. \quad (19)$$

We use the same notation in both frames because the relevant components  $H_{\omega\parallel}$ ,  $H_{\omega\perp}$ ,  $D_\parallel$ , and  $D_\perp$  remain invariant under transition from the one frame to another.

Let us find the co-rotating frequency  $\omega_c$ . By assumption all  $\mathbf{P}_\omega$ , and consequently  $\mathbf{M}$ , stay in the co-rotating plane. Therefore we can decompose

$$\mathbf{M} = b \mathbf{B} + \omega_c \mathbf{D} \quad (20)$$

and rewrite the EOM of Eq. (9) as

$$\partial_t \mathbf{D} = \omega_c \mathbf{B} \times \mathbf{D}. \quad (21)$$

Projecting Eq. (20) on the transverse plane we find  $\omega_c = M_\perp/D_\perp$  or explicitly

$$\omega_c = \frac{\int_{-\infty}^{+\infty} d\omega s_\omega \omega P_{\omega\perp}}{\int_{-\infty}^{+\infty} d\omega s_\omega P_{\omega\perp}} = \frac{\int_{-\infty}^{+\infty} d\omega s_\omega \omega P_{\omega\perp}}{D_\perp}. \quad (22)$$

When  $\mu \rightarrow \infty$  and all  $\mathbf{P}_\omega$  are aligned, this is identical with the synchronization frequency Eq. (11).

## B. Adiabatic solution in terms of sum rules

Initially when  $\mu$  is very large, all individual Hamiltonians are essentially aligned with  $\mathbf{D}$ . In turn,  $\mathbf{D}$  is aligned with the weak-interaction direction if initially all polarization vectors  $\mathbf{P}_\omega$  are aligned with that direction. In other words, all neutrinos are prepared in interaction eigenstates and initially  $\mathbf{P}_\omega \propto \mathbf{H}_\omega$ . The adiabatic evolution would imply that if  $\mu$  changes slowly enough,  $\mathbf{P}_\omega$  follows  $\mathbf{H}_\omega(\mu)$  and therefore remains aligned with  $\mathbf{H}_\omega(\mu)$  at later times as well. So the adiabatic solution of the EOMs for our initial condition is given by

$$\mathbf{P}_\omega(\mu) = \hat{\mathbf{H}}_\omega(\mu) P_\omega, \quad (23)$$

where  $P_\omega = |\mathbf{P}_\omega|$  and  $\hat{\mathbf{H}}_\omega \equiv \mathbf{H}_\omega/|\mathbf{H}_\omega|$  is a unit vector in the direction of the Hamiltonian.

According to the solution Eq. (23) all  $\mathbf{P}_\omega$  being confined to the co-rotating plane evolve in this frame according to the change of  $\mu$ . The solution is implicit since  $\hat{\mathbf{H}}_\omega$  depends via  $\mathbf{D} = \mathbf{D}(\mathbf{P}_\omega)$  on the polarization vectors:

$$\mathbf{H}_\omega = \mathbf{H}_\omega(\mathbf{P}_\omega), \quad \mathbf{P}_\omega = P_\omega(\hat{\mathbf{H}}_\omega). \quad (24)$$

We will see that there is a consistent solution which satisfies these relations. Notice that by imposing the “alignment” condition Eq. (23) on  $\mathbf{P}_\omega$ , we also restrict the Hamiltonian, since  $\mathbf{H}_\omega$  depends on  $\mathbf{P}_\omega$ .

Let us find explicit solutions  $P_{\omega\parallel}$  and  $P_{\omega\perp}$ . Since  $P_\omega$  is conserved and simply the spectrum of neutrinos given by the initial condition, we only need to find the Hamiltonians Eq. (19). They, in turn, are completely determined by  $\omega_c(\mu)$  and  $D_\perp(\mu)$  because  $D_{\omega\parallel}$  is known to be constant as determined by the lepton number. In other words, we need to find self-consistent results for  $\omega_c(\mu)$  and  $D_\perp(\mu)$ , the component transverse to  $\mathbf{B}$ , for a given  $D_\parallel$ .

The implicit adiabatic solution Eq. (23) gives us two equations for each  $\omega$  which we use to find  $\omega_c(\mu)$  and  $D_\perp(\mu)$ . Projecting Eq. (23) onto the perpendicular and parallel directions with respect to  $\mathbf{B}$  provides

$$\begin{aligned} P_{\omega\perp} &= \frac{H_{\omega\perp}}{H_\omega} P_\omega, \\ P_{\omega\parallel} &= \frac{H_{\omega\parallel}}{H_\omega} P_\omega. \end{aligned} \quad (25)$$

From Eq. (19) we infer

$$\begin{aligned} H_{\omega\perp} &= \mu D_{\perp}, \\ H_{\omega\parallel} &= \omega - \omega_c + \mu D_{\parallel}, \end{aligned} \quad (26)$$

so that

$$P_{\omega\parallel} = \frac{(\omega - \omega_c + \mu D_{\parallel}) P_{\omega}}{\sqrt{(\omega - \omega_c + \mu D_{\parallel})^2 + (\mu D_{\perp})^2}}, \quad (27)$$

$$P_{\omega\perp} = \frac{\mu D_{\perp} P_{\omega}}{\sqrt{(\omega - \omega_c + \mu D_{\parallel})^2 + (\mu D_{\perp})^2}}. \quad (28)$$

Integration of these equations over  $s_{\omega} d\omega$  gives us

$$D_{\parallel} = \int_{-\infty}^{+\infty} d\omega s_{\omega} \frac{(\omega - \omega_c + \mu D_{\parallel}) P_{\omega}}{\sqrt{(\omega - \omega_c + \mu D_{\parallel})^2 + (\mu D_{\perp})^2}}, \quad (29)$$

$$1 = \int_{-\infty}^{+\infty} d\omega s_{\omega} \frac{P_{\omega}}{\sqrt{[(\omega - \omega_c)/\mu + D_{\parallel}]^2 + D_{\perp}^2}}. \quad (30)$$

For a given  $D_{\parallel}$  and spectrum  $P_{\omega}$ , we can determine  $\omega_c$  and  $D_{\perp}$  from Eqs. (29) and (30) for any  $\mu$  and thus find explicit solutions.

Equations (29) and (30) can be considered as sum rules—integrals over frequencies that should be equal to certain conserved numbers. They can be added to each other with various factors so that one can rewrite them in different forms depending on convenience. For example, Eq. (29) can be rewritten with the use of Eq. (30) as

$$\omega_c = \int_{-\infty}^{+\infty} d\omega s_{\omega} \frac{\omega P_{\omega}}{\sqrt{[(\omega - \omega_c)/\mu + D_{\parallel}]^2 + D_{\perp}^2}} \quad (31)$$

which coincides with the form derived in our previous paper [14].

While different forms of the sum rules are equivalent, their limiting behavior for  $\mu \rightarrow 0$  or  $\mu \rightarrow \infty$  is not always equally manifest. For example, the physically intuitive expression Eq. (22) for  $\omega_c$  is valid only for  $D_{\perp}(\mu) \neq 0$  while for  $D_{\perp} = 0$  it has a 0/0 feature. On the other hand, Eq. (31) for  $\mu \rightarrow \infty$  is equivalent to the synchronization frequency Eq. (11) without any ambiguity.

Inserting the solution Eq. (23) into the EOM Eq. (13) we obtain

$$\partial_t \mathbf{H}_{\omega}(\mu) = 0 \quad (32)$$

which is satisfied exactly if  $\partial_t \mu = 0$  and  $\partial_t \mathbf{D} = 0$ . That is, the medium has constant neutrino density and the difference vector does not change. The latter is satisfied when all polarization vectors stay unchanged, but this may not be the only possibility. We will call this self-consistent solution the “static solution.” For a slowly varying density the condition Eq. (32) is only approximately satisfied. As in the usual MSW case, Eq. (23) provides an approximate solution of the EOMs, when the dependence of the Hamiltonian on time is negligible. The adiabatic solution

(the lowest order term in the adiabatic perturbation theory) is given by a continuous set of static (instantaneous) solutions.

Let us comment on the static solution. It consists of all  $\mathbf{P}_{\omega}$  being confined to the co-rotating plane. The motion of all polarization vectors is limited to a common precession around  $\mathbf{B}$  with frequency  $\omega_c$ , each of them having a different zenith angle relative to  $\mathbf{B}$ . Duan et al. have termed this form of motion the “pure precession mode” [12]. In contrast to the usual MSW case, the static solution implies an additional condition  $\mathbf{D} = \text{const.}$  which does not mean in general that the individual polarization vectors are static. Another issue is the stability of the solution since  $\mathbf{D}$  is a dynamical system and not a rigid vector. Furthermore, separate equalities  $\partial_t \mu = 0$  and  $\partial_t \mathbf{D} = 0$  may not be the only solutions of Eq. (32). Our numerical studies show, however, that the static solutions are not only self-consistent, but also stable.

For every spectrum  $P_{\omega}$  the pure precession solutions are characterized by the two parameters  $D_{\parallel}$  and  $\mu$ . For  $\mu \rightarrow \infty$  all Hamiltonians are aligned and thus all  $\mathbf{P}_{\omega}$  are aligned as well, provided that they are in a pure precession mode. Assuming the neutrinos are produced in interaction eigenstates, all  $\mathbf{P}_{\omega}$  are tilted relative to  $\mathbf{B}$  with twice the effective mixing angle so that

$$D_{\parallel} = \cos 2\theta_{\text{eff}} \int_{-\infty}^{+\infty} d\omega s_{\omega} P_{\omega}. \quad (33)$$

In this sense we have, for every spectrum  $P_{\omega}$ , a two-parameter family of static solutions given in terms of  $\cos 2\theta_{\text{eff}}$  and  $\mu$  or equivalently, in terms of  $D_{\parallel}$  and  $\mu$ .

### C. Split frequency

In the limit  $\mu \rightarrow \infty$  all polarization vectors are aligned with each other in a direction given by the choice of  $\cos 2\theta_{\text{eff}}^{\infty}$ , i.e., by the initial condition. In the opposite limit,  $\mu \rightarrow 0$ , the solution is given by

$$\mathbf{H}_{\omega} \rightarrow (\omega - \omega_c^0) \mathbf{B}, \quad (34)$$

where  $\omega_c^0 \equiv \omega_c(\mu \rightarrow 0)$ . All Hamiltonians and thus all  $\mathbf{P}_{\omega}$  with  $\omega > \omega_c^0$  are aligned with  $\mathbf{B}$ , whereas those with  $\omega < \omega_c^0$  are anti-aligned. Therefore, we have a spectral split at the frequency

$$\omega_{\text{split}} = \omega_c^0 \quad (35)$$

which usually is not equal to zero.

$D_{\perp} = 0$  because in the end all polarization vectors are (anti)aligned with  $\mathbf{B}$ . Moreover, for  $\mu \rightarrow 0$  Eq. (29) approaches a well-defined limit,

$$\begin{aligned} D_{\parallel} &= \int_{-\infty}^{+\infty} d\omega s_{\omega} \frac{(\omega - \omega_{\text{split}}) P_{\omega}}{\sqrt{(\omega - \omega_{\text{split}})^2}} \\ &= \int_{-\infty}^{+\infty} d\omega s_{\omega} s_{\omega - \omega_{\text{split}}} P_{\omega}. \end{aligned} \quad (36)$$

For our usual case of an excess neutrino flux ( $D_{\parallel} > 0$  and  $\omega_{\text{split}} > 0$ ) this equation is identical with

$$D_{\parallel} = \int_{-\infty}^0 P_{\omega} d\omega - \int_0^{\omega_{\text{split}}} P_{\omega} d\omega + \int_{\omega_{\text{split}}}^{+\infty} P_{\omega} d\omega. \quad (37)$$

The first term enters with a positive sign because antineutrinos enter lepton number with a negative sign, but are now oriented opposite to  $\mathbf{B}$ , the next term has a negative sign because it represents those neutrino modes that in the end are oriented against  $\mathbf{B}$ , and the third term has a positive sign because it represents neutrinos with orientation along  $\mathbf{B}$ .

In practice we are mostly interested in the application to SN physics where the effective mixing angle is small. In this case there are other intuitive ways to state the condition of lepton-number conservation and to determine the split frequency. We can rewrite the definition of  $\mathbf{D}$  in Eq. (7) for  $\theta_{\text{eff}}^{\infty} \approx 0$  in the following explicit form

$$D_{\parallel} \approx - \int_{-\infty}^0 P_{\omega} d\omega + \int_0^{\omega_{\text{split}}} P_{\omega} d\omega + \int_{\omega_{\text{split}}}^{+\infty} P_{\omega} d\omega. \quad (38)$$

Now we have two equations, Eq. (37) and Eq. (38), for integrals over different parts of spectra. The first equation gives us the total lepton number of the initial state where antineutrinos enter with a negative sign, neutrinos with a positive sign. The second equation simply reflects that all modes below  $\omega_{\text{split}}$  were flipped.

Subtracting or adding these equations eliminates different parts of the spectrum and reveals

$$\int_{-\infty}^0 d\omega P_{\omega} = \int_0^{\omega_{\text{split}}} d\omega P_{\omega} \quad (39)$$

and

$$D_{\parallel} = \int_{\omega_{\text{split}}}^{+\infty} d\omega P_{\omega}. \quad (40)$$

Equation (39) has the interpretation that all antineutrinos ( $-\infty < \omega < 0$ ) are converted and therefore to conserve lepton number the same number of neutrinos should be converted. From the continuity in  $\omega$  we infer that those are neutrinos with frequencies with  $0 < \omega < \omega_{\text{split}}$ . Equation (40) has the interpretation that the net lepton charge of the system should be determined by the high frequency part of the neutrino spectrum.

For the case of a dominant antineutrino flux ( $\alpha > 1$ ) we have  $D_{\parallel} < 0$ , the split frequency is negative and the spectral split occurs in the antineutrino channel. Now all modes with frequencies above  $\omega_{\text{split}}$  are converted whereas the modes with negative  $\omega$  below  $\omega_{\text{split}}$  stay unchanged. The sum rule for the determination of  $\omega_{\text{split}}$  now becomes

$$D_{\parallel} = - \int_{-\infty}^{\omega_{\text{split}}} d\omega P_{\omega} + \int_{\omega_{\text{split}}}^0 d\omega P_{\omega} - \int_0^{+\infty} d\omega P_{\omega}. \quad (41)$$

Instead of Eq. (40) we get

$$D_{\parallel} = - \int_{\infty}^{\omega_{\text{split}}} d\omega P_{\omega}. \quad (42)$$

The net charge now comes from negative frequencies. So in this case the entire neutrino flux and high energy part of the antineutrino flux change flavor whereas the low energy antineutrino flux is unchanged.

## IV. SOLUTIONS FOR NEUTRINOS

### A. Box spectrum

As a first example for explicit adiabatic solutions we consider the simplest possible case where neutrino-neutrino interactions lead to a spectral split in the adiabatic limit: An ensemble consisting of neutrinos only ( $\alpha = 0$ ), no antineutrinos and no ordinary matter. Now  $\mathbf{D} = \mathbf{P}$  and correspondingly  $D_{\parallel} = P_{\parallel}$  and  $D_{\perp} = P_{\perp}$ . Of course, this is an abstract example meant to illustrate the general phenomenon. In subsequent sections we will turn to realistic situations relevant in a SN.

We use a flat distribution of oscillation frequencies with the average  $\omega_0$ , i.e., the box-like spectrum

$$P_{\omega} = \begin{cases} (2\omega_0)^{-1} & \text{for } 0 \leq \omega \leq 2\omega_0, \\ 0 & \text{otherwise.} \end{cases} \quad (43)$$

With  $P_{\parallel}$  the conserved projection of  $\mathbf{P}$  on the  $\mathbf{B}$ -direction we find from Eqs. (31) and (37), recalling that Eqs. (39) and (40) are valid for  $\theta_{\text{eff}}^{\infty} \approx 0$ ,

$$\omega_c = \omega_0 \times \begin{cases} 1 & \text{for } \mu \rightarrow \infty, \\ (1 - P_{\parallel}) & \text{for } \mu = 0. \end{cases} \quad (44)$$

Notice that for  $P_{\parallel} = 0$ , corresponding to maximal initial mixing, the frequency  $\omega_c = \omega_0$  is constant for the entire evolution. For  $P_{\parallel} = 1$  (vanishing mixing angle) we have  $\omega_c = 0$ , corresponding to the absence of any flavor evolution. We will see in Sec. V that in the presence of antineutrinos even a very small mixing angle leads to a large effect, whereas here we need to assume a non-zero mixing angle to obtain something visible.

In Fig. 3 we show the initial and final distribution  $P_{\omega\parallel}$  for the example  $P_{\parallel} = 0.5$ , so that according to Eq. (44)  $\omega_{\text{split}} = \omega_c^0 = 0.5\omega_0$ . The dotted line indicates the final distribution in the adiabatic limit, the solid line is the result of a numerical example with  $\mu(t)$  from Eq. (5) with  $\tau = (0.03\omega_0)^{-1}$ . The spectral split indeed becomes sharper with increasing  $\tau$  (increasing adiabaticity) as discussed in more detail in Sec. VII.

We may also follow the evolution of the individual polarization vectors. In Fig. 4 we show  $P_{\omega\parallel}$  for 51 equally spaced modes as a function of  $\omega_0/\mu$  for the example of Fig. 3. At first, all of them begin with the common starting value  $P_{\omega\parallel} = 0.5$ . Later they spread out and eventually split, some of them approaching +1 and the others

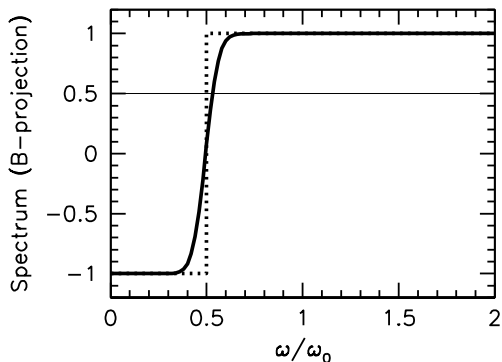


FIG. 3: Initial (thin line) and final (thick line) neutrino spectra for the example of Eq. (43). Dotted: fully adiabatic. Solid: numerical example with  $\tau = (0.03\omega_0)^{-1}$  in Eq. (5).

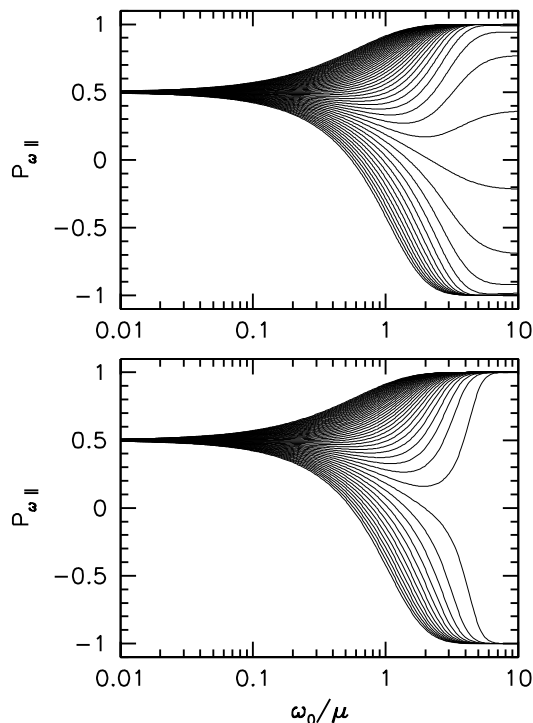


FIG. 4: Evolution of 51 equally spaced modes for the same example as in Fig. 3. *Top*: Numerical solution with  $\tau = (0.03\omega_0)^{-1}$ . *Bottom*: Adiabatic solution derived in Sec. IV B.

$-1$  as predicted. Some of them first move down and then turn around as a result of  $\omega_c$  changing as a function of time. As a result of imperfect adiabaticity, a few modes do not reach  $\pm 1$  but get frozen before this destination.

### B. Analytic solution

In the adiabatic limit, the same results follow from our explicit solution of the EOMs. For the box spectrum Eq. (43) the integrals Eqs. (29) and (30) are easily per-

formed. After some transformations we find

$$\begin{aligned} \frac{\omega_c}{\omega_0} &= 1 + P_{\parallel} \left( \frac{1}{\kappa} - \frac{e^{\kappa} + e^{-\kappa}}{e^{\kappa} - e^{-\kappa}} \right), \\ P_{\perp} &= \sqrt{1 - P_{\parallel}^2} \frac{2\kappa}{e^{\kappa} - e^{-\kappa}}, \end{aligned} \quad (45)$$

where

$$\kappa \equiv \omega_0/\mu. \quad (46)$$

For  $\mu \rightarrow \infty$  and  $\mu \rightarrow 0$  the limits of  $\omega_c$  agree with the results predicted in Eq. (44). For  $\mu \rightarrow \infty$  we have  $P_{\perp} = (1 - P_{\parallel}^2)^{1/2}$ , representing the initial condition  $P = 1$ . For  $\mu \rightarrow 0$  we find  $P_{\perp} = 0$ , corresponding to all polarization vectors either aligned or anti-aligned with  $\mathbf{B}$ .

For our example with  $P_{\parallel} = 0.5$  we show  $\omega_c(\kappa)$  and  $P_{\perp}(\kappa)$  in Fig. 5. According to Eq. (45),  $\omega_c$  decreases monotonically with increasing  $\kappa$  from  $\omega_c = \omega_0$  to  $\omega_c = \omega_{\text{split}} = 1 - P_{\parallel} = 0.5$ . The transverse component  $P_{\perp}$  decreases from  $(1 - P_{\parallel}^2)^{1/2} = \sqrt{0.75} = 0.866$  down to 0. With Eq. (27) the analytic results provide exact adiabatic solutions for the  $\parallel$ -component of the polarization-vector spectrum. In the bottom panel of Fig. 4 we show the evolution for 51 equally spaced modes in analogy to the numerical result shown in the upper panel. The agreement for not very small  $\mu$  is striking, thus confirming the correctness of our picture based on the adiabatic evolution in the co-rotating frame. The curves obtained in the adiabatic approximation and by numerical solution of the original evolution equations do not agree for the modes

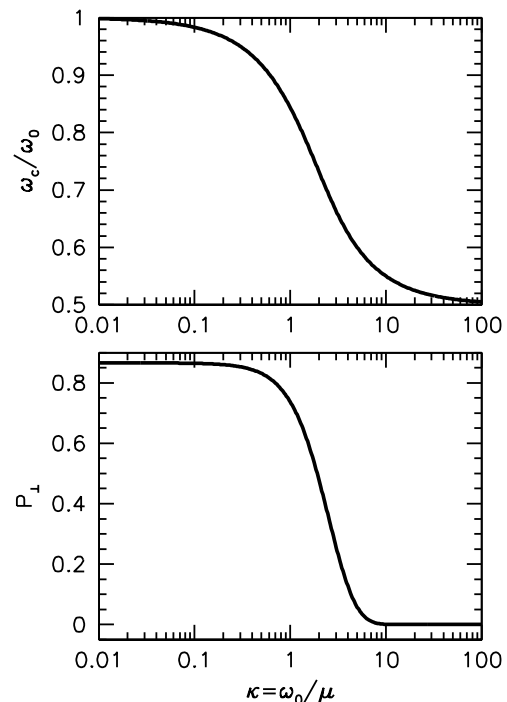


FIG. 5: Analytic results for  $\omega_c(\kappa)$  and  $P_{\perp}(\kappa)$  according to Eq. (45) with the initial condition  $P_{\parallel} = 0.5$ .



close to the split ( $\omega \approx \omega_{\text{split}}$ ) at low neutrino densities ( $\mu < \omega_0$ ) where the evolution becomes non-adiabatic.

Figure 4 shows that the trajectories of different modes literally split in the course of evolution, giving us another (dynamical) motivation for the term “spectral split” to describe the phenomenon.

It is remarkable that the split is essentially complete only for  $\omega_0/\mu \gtrsim 7$  or  $\mu \lesssim 0.15\omega_0$ . In other words, the overall motion remains collective in the sense of all polarization vectors precessing in a common plane for a surprisingly small value of  $\mu$ , even for imperfect adiabaticity as in the upper panel of Fig. 4.

Actually for any value of  $\mu$ , no matter how small, our adiabatic case is an exact solution of the EOMs where all polarization vectors precess in a common plane. Of course, for very small  $\mu$  their angles relative to the positive or negative  $\mathbf{B}$  direction are exponentially small, but conceptually this is still a collective motion. In the perfectly adiabatic case, collectivity is never lost. Instead, the polarization vectors orient themselves in the positive or negative  $\mathbf{B}$ -direction.

If  $\mu$  were to switch off suddenly, the transverse component of the overall  $\mathbf{P}$  disappears by kinematical decoherence because all  $\mathbf{P}_\omega$  precess with different frequencies. In the perfectly adiabatic case, the transverse component disappears because all individual  $\mathbf{P}_\omega$  (anti)align themselves with  $\mathbf{B}$  while remaining in a common plane. There is never any kinematical decoherence caused by differences of precession frequencies between different modes. The persistence of collectivity for arbitrarily small  $\mu$  is the most surprising aspect of this system.

### C. Spectral cross-over

At the neutrino sphere in a SN it is expected that the  $\nu_e$  flux dominates for low energies and the  $\nu_x$  flux for high energies. This would be the case, for example, if both species are emitted with equal luminosities but different average energies. In this case the initial  $\mathbf{P}_\omega$  are either aligned or anti-aligned with the flavor direction. In the previous discussion we must then be careful about absolute signs of the various projections of the polarization vectors.

An important difference occurs in Eq. (23) because  $\mathbf{P}_\omega$  can be anti-aligned with  $\hat{\mathbf{H}}_\omega$  so that  $P_\omega$  should be taken negative for those modes that initially contain the “wrong” flavor. The final state of these modes will be opposite from where they would have ended if they had been occupied with the “correct” flavor.

The final spectrum is again determined by flavor lepton-number conservation. Imagine that the low- $\omega$  modes are initially in the other flavor, corresponding to a fraction  $\xi$  of all modes, and assume a box spectrum (thin line in the top left panel of Fig. 6). These modes must now end up at  $P_{\omega\parallel} = +1$ , affecting the net flavor lepton number. The modes above  $\omega_{\text{split}}$  also must end up at  $+1$ , whereas intermediate ones end up at  $-1$ . It is now easy

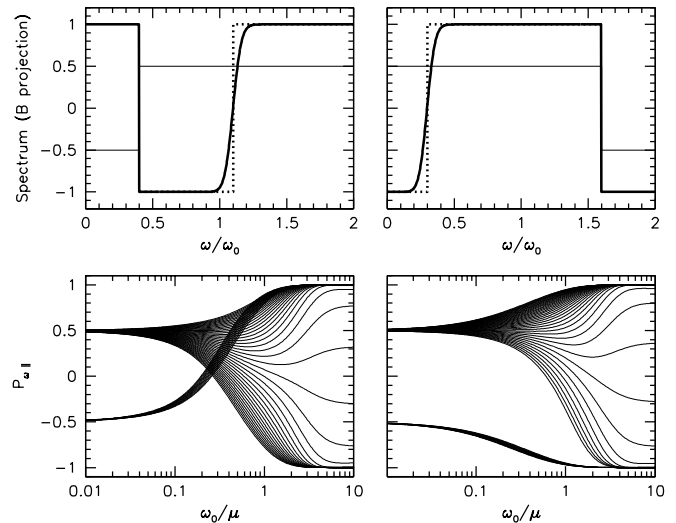


FIG. 6: Examples for crossed-over neutrino spectra. *Top:* Thin solid: initial. Thick dotted: adiabatic final. Thick solid: numerical final with  $\tau = (0.03\omega_0)^{-1}$  in Eq. (5). *Bottom:* Numerical evolution of 51 equally spaced modes.

to work out that in the end ( $\mu \rightarrow 0$ )

$$\omega_{\text{split}} = \omega_0 [1 - \cos \beta + 2\xi (1 + \cos \beta)], \quad (47)$$

where  $\beta$  is the initial angle between  $\mathbf{B}$  and  $\mathbf{P}$ . For  $\xi = 0.2$  and  $\cos \beta = 0.5$  we thus find  $\omega_{\text{split}} = 1.1\omega_0$ . In this way we predict for the example of Fig. 6 (left column) the final spectrum indicated by a thick dotted line. Numerically we find the thick solid line.

The split at  $\omega_{\text{split}}$  is somewhat washed out because the evolution is not fully adiabatic. On the other hand, the transition at the initial spectral cross over remains sharp because the end state of those modes depends only on the initial sign of  $P_\omega$ , but otherwise we are in an adiabatic regime of the spectrum.

In the bottom panel we show the familiar pattern of the  $P_{\omega\parallel}$  evolution with the novel feature that the modes that were initially in the other flavor cross over to  $P_{\omega\parallel} = +1$ .

In the right-hand panels of Fig. 6 we show an analogous example where the high- $\omega$  part of the initial spectrum is crossed over. The explanation is analogous.

## V. NEUTRINOS AND ANTINEUTRINOS

### A. Solution for the double-box spectrum

As a next case towards a more complete understanding we include antineutrinos in our model, upholding the condition that all polarization vectors  $\mathbf{P}_\omega$ , now with frequencies in the range  $-\infty < \omega < +\infty$ , initially point in the same direction. We assume that the fraction of antineutrinos is  $\alpha < 1$  of the neutrinos. We will always assume the inverted mass hierarchy so that a large flavor

transformation effect is caused by the instability of the inverted flavor pendulum [11, 16].

As a generic example we extend the box spectrum of the previous section to include antineutrinos. To be specific, we assume a double-box spectrum of equal width, but different height for the neutrinos and antineutrinos:

$$P_\omega = \frac{1}{2\omega_0} \times \begin{cases} \alpha & \text{for } -2\omega_0 \leq \omega \leq 0, \\ 1 & \text{for } 0 < \omega \leq 2\omega_0, \\ 0 & \text{otherwise.} \end{cases} \quad (48)$$

We will assume  $\alpha = 0.7$  as a standard case.

The thin line in Fig. 7 represents this initial spectrum where antineutrinos are represented with negative frequencies. Using the same arguments as in the neutrino-only case, in the co-rotating frame the antineutrinos are modes with even more negative frequencies than those neutrinos with  $\omega < \omega_{\text{split}}$ . Therefore, they should simply reverse their direction. This is borne out by the numerical final spectra in Fig. 7 (thick solid line). The adiabatic limit (thick dotted line) is again explained by the conservation of flavor lepton number.

Next we consider the evolution of the individual modes. In the upper panels of Fig. 8 we show  $P_{\omega\parallel}(\mu)$  for neutrinos and in the lower panel for antineutrinos. As expected, they evolve at first collectively and both global polarization vectors tilt against the  $\mathbf{B}$  direction, the familiar result of neutrino-neutrino refraction in the inverted hierarchy case. Later the modes separate to produce the final spectrum. In Fig. 8 we juxtapose the direct numerical solution of the EOMs, assuming  $\sin 2\theta_{\text{eff}}^\infty = 0.05$  and a not very adiabatic  $\tau = (0.1\omega_0)^{-1}$ , with the fully adiabatic solution for  $\sin 2\theta_{\text{eff}}^\infty = 0$  (right panels).

We could have illustrated this case by using the same length for the  $\mathbf{P}_\omega$  for both neutrinos and antineutrinos, but occupying only 70% of the antineutrino modes. In this alternative double-box case we could have shown the evolution of all modes in a single plot because the antineutrino modes seamlessly join the neutrino modes.

A new feature of the left panels of Fig. 8 is the “wig-

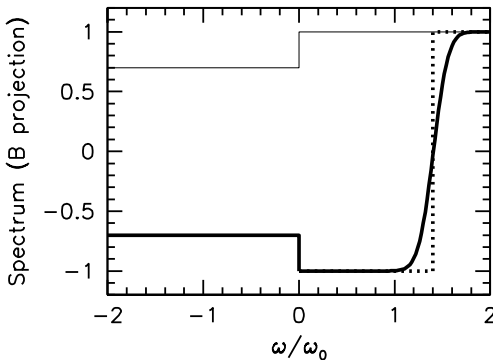


FIG. 7: Neutrino spectra for an initial box spectrum with 70% antineutrinos and  $\sin 2\theta_{\text{eff}}^\infty = 0.05$ . Negative frequencies correspond to antineutrinos. Thin line: initial. Thick dotted: final adiabatic. Thick solid: numerical example with  $\tau = (0.1\omega_0)^{-1}$  in Eq. (5).

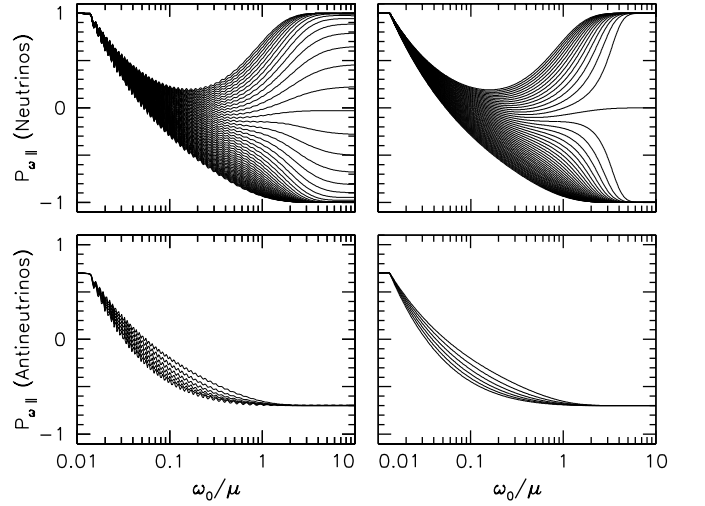


FIG. 8:  $P_{\omega\parallel}(\mu)$  for individual modes for the case of neutrinos plus antineutrinos. *Left*: Numerical solution from the EOMs as in our previous paper [14] for  $\sin 2\theta_{\text{eff}}^\infty = 0.05$ . *Right*: Adiabatic solution for  $\sin 2\theta_{\text{eff}}^\infty = 0$ . In each case neutrinos with 51 modes (top) and antineutrinos with 6 modes (bottom).

gles” in the curves that stem from the nutation of the global flavor pendulum. We will return to this issue later but for now only note that the wiggles disappear in the numerical solution if we take the scale parameter  $\tau$  very large, much larger than is realistic in the SN context. In this case the split would be extremely sharp. In order to show a not fully adiabatic solution we have here used parameters that do not have too many nutation periods (relatively small  $\tau$ ) and where the nutation depth is not too large (mixing angle not too small) or else the plot would be too cluttered. In any case, there are no nutations in an “extremely adiabatic” situation which for the moment we focus on.

The adiabatic solution for the individual modes shown in the right-hand panels of Fig. 8 were found from solving our sum rules Eqs. (29) and (30) numerically. The curves  $\omega_c(\mu)$  and  $D_\perp(\mu)$  for a vanishing mixing angle are shown as thick solid lines in Fig. 9. It shows interesting new features compared to the neutrino-only case. For  $\mu \rightarrow \infty$  we have  $D_\perp = 0$  due to the assumption of a vanishing mixing angle. The precession frequency corresponds to the expected synchronization frequency. However, for decreasing  $\mu$  the precession frequency increases up to an apparent cusp, and then decreases eventually down to the expected split frequency. At the cusp,  $D_\perp$  begins to deviate from zero whereas  $D_\perp = 0$  for  $0 < \mu^{-1} < \mu_{\text{cusp}}^{-1}$ . In other words, the cusp marks the neutrino-neutrino interaction strength where the polarization vectors begin to tilt away from the  $\mathbf{B}$  direction and begin to spread in the zenith-angle direction.

For comparison we show, as a thin line, the same result for a large initial mixing angle,  $\sin 2\theta_{\text{eff}}^\infty = 0.5$ , implying that initially  $D_\perp = (1 - \alpha) \sin 2\theta_{\text{eff}}^\infty = 0.15$ . The curve is qualitatively similar but does not show any cusps or

kinks. Notice that for  $\omega_c > 2\omega_0$  the co-rotation frequency is above the maximal frequency of the spectrum for  $\kappa < 1$ . Therefore, a true split of the modes (in contrast to a zenith-angle spread) only starts when  $\omega_c = 2\omega_0$ , that is at  $\kappa = 1$ . Apparently the dependences in Fig. 9 differ from that in Fig. 5 for pure neutrino case.

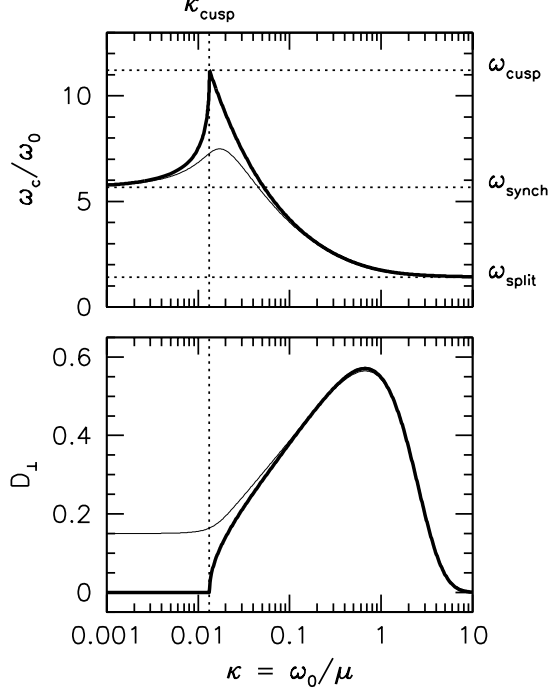


FIG. 9: Numerical solution of Eqs. (29) and (30) for the double-box spectrum of neutrinos plus antineutrinos with  $\alpha = 0.7$  and  $\sin 2\theta_{\text{eff}}^\infty = 0$ . The vertical dotted line indicates  $\kappa_{\text{cusp}} = 0.013340$  below which the system is perfectly synchronized. The horizontal dotted lines indicate  $\omega_{\text{synch}} = \omega_c^\infty = (17/3)\omega_0$  and  $\omega_{\text{split}} = \omega_c^0 = (14/10)\omega_0$ . The thin solid line is the same case with  $\sin 2\theta_{\text{eff}}^\infty = 0.5$ .

### B. Properties of the pure precession mode

Before turning to more physical interpretations of these features, notably the cusp, we first investigate some mathematical properties of these solutions. For the double-box spectrum, the sum rules can be evaluated analytically. Eq. (30) gives

$$\frac{(y_+ + \sqrt{y_+^2 + D_\perp^2})(y_- + \sqrt{y_-^2 + D_\perp^2})^\alpha}{(y_0 + \sqrt{y_0^2 + D_\perp^2})^{1+\alpha}} = e^{2\kappa}, \quad (49)$$

where  $y_\pm = y_0 \pm 2\kappa$  and  $y_0 \equiv D_\parallel - (\omega_c/\omega_0)\kappa$ . The integration of Eq. (29) leads to

$$\sqrt{y_+^2 + D_\perp^2} + \alpha\sqrt{y_-^2 + D_\perp^2} - (1+\alpha)\sqrt{y_0^2 + D_\perp^2} = 2\kappa D_\parallel. \quad (50)$$

Practically it is not possible to extract  $D_\perp$  and  $\omega_c$  as functions of  $\mu$  in closed form for generic values of parameters.

In a SN, the most interesting case is  $\sin 2\theta_{\text{eff}}^\infty \approx 0$ , where  $D_\parallel = 1 - \alpha$ . This extreme case entails a number of simplifications, but also a number of subtleties. It is easy to find  $\omega_c(\kappa)$  for special values of  $\kappa$ .

#### 1. Synchronization frequency

From Eq. (11) we easily derive the initial common oscillation frequency, corresponding to the well-known synchronization frequency,

$$\omega_c^\infty = \omega_{\text{synch}} = \omega_0 \frac{1 + \alpha}{1 - \alpha}. \quad (51)$$

For  $\alpha = \frac{7}{10}$  this is  $\omega_{\text{synch}} = \frac{17}{3}\omega_0 = 5.667\omega_0 > 2\omega_0$ . Therefore, initially  $\omega_c$  is “outside of the spectral box,” i.e., all neutrino and antineutrino modes have negative frequencies in the co-rotating frame.

#### 2. Split frequency

Later the modes split and the final split frequency at  $\mu = 0$  is found from  $\nu_e$  number conservation to be

$$\omega_{\text{split}} = \omega_0(1 - D_z + \alpha) = \omega_0 2\alpha, \quad (52)$$

where we have used that for a very small mixing angle  $D_\parallel = 1 - \alpha$ . With  $\alpha = 0.7$  this is  $\omega_{\text{split}} = 1.4\omega_0$  in agreement with Fig. 7. Independently of the choice of  $\alpha$ , the final  $\omega_{\text{split}}$  always lies “within the box” because  $\omega_0 2\alpha < 2\omega_0$  so that a split always occurs. In the end  $D_\perp = 0$  due to the (anti)alignment of all polarization vectors with **B**.

#### 3. Cusp

A final special quantity is the strength of the neutrino-neutrino interaction where the system exits the synchronization regime and enters the “bipolar regime.” This transition is infinitely abrupt when  $\sin 2\theta_{\text{eff}}^\infty = 0$  and corresponds to the cusp in  $\omega_c(\kappa)$  shown in Fig. 9.

For  $0 < \kappa < \kappa_{\text{cusp}}$  we note that  $D_\perp = 0$  solves Eq. (50) identically. Equation (49) can be written in the form

$$(1 - u)^\alpha(1 + u) = e^{2\kappa}, \quad (53)$$

where

$$u = \frac{2\kappa}{D_\parallel - \kappa\omega_c/\omega_0}. \quad (54)$$

At  $\kappa = \kappa_{\text{cusp}}$  the function  $\omega_c(\kappa)$  appears to have a vertical tangent. If this is true,  $u(\kappa)$  also should have a vertical tangent or  $\kappa(u)$  should have a horizontal one.

Equation (53) is trivially inverted to provide an explicit expression for  $\kappa(u)$ . Using the condition  $d\kappa/du = 0$  we find  $u_{\text{cusp}}$ . Sticking this back into  $\kappa(u)$  we obtain

$$\begin{aligned}\kappa_{\text{cusp}} &= \frac{1}{2} \left[ \log \left( \frac{2}{1+\alpha} \right) + \alpha \log \left( \frac{2\alpha}{1+\alpha} \right) \right] \\ &= 0.01330 \quad (\text{for } \alpha = 0.7).\end{aligned}\quad (55)$$

The co-rotation frequency at the cusp is found to be

$$\begin{aligned}\frac{\omega_{\text{cusp}}}{\omega_0} &= \frac{1+\alpha}{\kappa_{\text{cusp}}} - 2 \frac{1+\alpha}{1-\alpha} \\ &= 11.2148 \quad (\text{for } \alpha = 0.7).\end{aligned}\quad (56)$$

The values of  $\kappa_{\text{cusp}}$  and  $\omega_{\text{cusp}}$  are in perfect agreement with the numerical result shown in Fig. 8, thus confirming that in the cusp  $\omega_c$  has a vertical tangent.

We observe that Eqs. (53) and (54) allow us to find the curve  $\omega_c(\kappa)$  analytically in parametric form, i.e., we can extract a pair of functions  $\omega_c(u)$  and  $\kappa(u)$ . One easily shows that the function  $\kappa(\omega_c)$  does not end at the cusp, but rather is well defined for  $\omega_{\text{synch}} \leq \omega_c < \infty$ . Turning this around, the function  $\omega_c(\kappa)$  is double valued for  $0 < \kappa < \kappa_{\text{cusp}}$ . We show the full solution in the upper panel of Fig. 10 where the unphysical part is continued as a dashed line.

In addition, we find numerically that the high- $\kappa$  branch also has a smooth continuation below the cusp. This

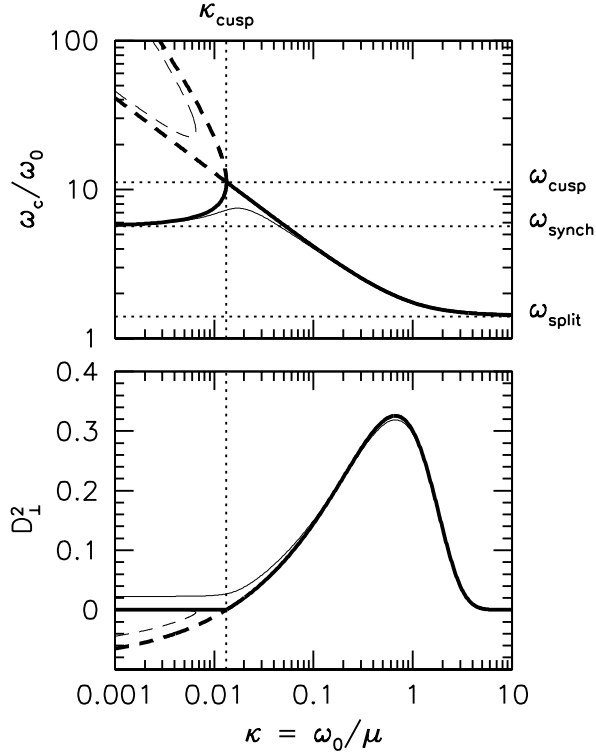


FIG. 10: Numerical solution of the sum rules Eqs. (29) and (30) as in Fig. 9, now including the unphysical solutions as dashed lines.

branch is also unphysical, corresponding to solutions with  $D_{\perp}^2 < 0$  shown as a dashed line in the lower panel of Fig. 10. The cusp actually corresponds to a cross-over of two solutions, although the physical solution indeed has a cusp.

The unphysical solutions persist for nonvanishing mixing angles. We show the complete numerical solutions for  $\sin 2\theta_{\text{eff}}^{\infty} = 0.5$  as thin lines in Fig. 10. The physical ( $D_{\perp}^2 > 0$ ) and unphysical ( $D_{\perp}^2 < 0$ ) solutions are now fully separated: there are no kinks or cusps as far as one can tell numerically.

For  $\sin 2\theta_{\text{eff}}^{\infty} = 0$  the physical solution has a cusp,  $D_{\perp} = 0$  is exact for the entire range  $0 < \kappa < \kappa_{\text{cusp}}$ , yet  $\omega_c$  varies in this range as a function of  $\kappa$ . These surprising features are more easily understood in a simpler case where one uses only two polarization vectors, one for neutrinos and one for antineutrinos, i.e., for a monochromatic neutrino spectrum. We will consider this example in Sec. VI and return there to a discussion of the  $\omega_c$  behavior.

## VI. TWO POLARIZATION VECTORS

As a last explicit example we study a system consisting of only two polarization vectors  $\mathbf{P}_1$  for neutrinos and  $\mathbf{P}_2$  for antineutrinos with  $P_1 = |\mathbf{P}_1| = 1$  and  $P_2 = |\mathbf{P}_2| = \alpha < 1$ . This example allows us to make a connection to the previous literature. Moreover, this system is a useful toy example to understand some of the peculiarities of the general neutrino-antineutrino system, notably the cusp feature in the common precession frequency  $\omega_c(\mu)$ . Finally, realistic spectra do not extend to infinite energies and therefore do not have a continuity in the region around  $\omega = 0$ . In this respect the two line-spectrum represent reality to a certain extend.

### A. Pure precession mode

According to Eq. (4) the equations of motion can be written in the form

$$\begin{aligned}\dot{\mathbf{P}}_1 &= +\omega_0 \mathbf{B} \times \mathbf{P}_1 + \mu \mathbf{P}_1 \times \mathbf{P}_2, \\ \dot{\mathbf{P}}_2 &= -\omega_0 \mathbf{B} \times \mathbf{P}_2 + \mu \mathbf{P}_1 \times \mathbf{P}_2.\end{aligned}\quad (57)$$

If  $\mathbf{P}_1$  and  $\mathbf{P}_2$  were free, both of them would precess with frequency  $\omega_0$ , but in opposite directions.

We first investigate the “pure precession mode” [12] of this system, at first without reference to adiabaticity, where both polarization vectors precess in a single plane around  $\mathbf{B}$ . If the vectors  $\mathbf{B}$ ,  $\mathbf{P}_1$  and  $\mathbf{P}_2$  are indeed in a single plane, then the velocity vectors being proportional to  $\mathbf{B} \times \mathbf{P}_1$ ,  $\mathbf{B} \times \mathbf{P}_2$  and  $\mathbf{P}_1 \times \mathbf{P}_2$  are all collinear. Let  $\vartheta_1$  and  $\vartheta_2$  be the angles between  $\mathbf{P}_1$  and  $\mathbf{P}_2$  and  $\mathbf{B}$ , respectively. If  $\mathbf{P}_1$  and  $\mathbf{P}_2$  are in the same plane, then both evolution equations can be reduced to the form  $\dot{\mathbf{P}}_i = \omega_c \mathbf{B} \times \mathbf{P}_i$

( $i = 1, 2$ ) with

$$\begin{aligned}\omega_c &= +\omega_0 + \mu \alpha \frac{\sin(\vartheta_2 - \vartheta_1)}{\sin \vartheta_1} \\ &= +\omega_0 + \mu \alpha \left( \frac{c_1 s_2}{s_1} - c_2 \right), \\ \omega_c &= -\omega_0 + \mu \frac{\sin(\vartheta_2 - \vartheta_1)}{\sin \vartheta_2} \\ &= -\omega_0 + \mu \left( c_1 - \frac{c_2 s_1}{s_2} \right),\end{aligned}\quad (58)$$

where we have used the notation  $c_1 \equiv \cos \vartheta_1$  and so forth. This is equivalent to Eq. (65) of Duan et al. [12].

Eliminating  $\mu \sin(\vartheta_2 - \vartheta_1)$  from the first form of these equations we find

$$\frac{\omega_c}{\omega_0} = \frac{s_1 + \alpha s_2}{s_1 - \alpha s_2}. \quad (59)$$

In the alignment case where  $\vartheta_1 = \vartheta_2$  we immediately reproduce

$$\frac{\omega_{\text{synch}}}{\omega_0} = \frac{1 + \alpha}{1 - \alpha} \quad (60)$$

for the synchronization frequency.

It is also trivial to eliminate  $\omega_c$  from the two equations in Eq. (58) and one finds

$$\kappa \equiv \frac{\omega_0}{\mu} = \frac{s_1 - \alpha s_2}{2} \left( \frac{c_1}{s_1} - \frac{c_2}{s_2} \right). \quad (61)$$

In the alignment case,  $\vartheta_1 = \vartheta_2$ , the pure precession mode requires  $\kappa = 0$  (or  $\mu \rightarrow \infty$ ).

### B. Alignment with Hamiltonians

It is surprising that for any two angles  $\vartheta_1$  and  $\vartheta_2$  one finds solutions  $\omega_c$  and  $\mu$  that permit a pure precession. Of course, suitable initial conditions are required to actually put the system into this mode. Demanding  $\mu$  to be positive (as it would for neutrino-neutrino interactions) implies some restrictions on the allowed angular ranges, but otherwise all combinations of angles are possible.

As a check of self-consistency we note that in the pure precession mode,  $\mathbf{P}_{1,2}$  do not move within the co-rotating frame. Therefore, in this frame their Hamiltonians must be collinear with  $\mathbf{P}_{1,2}$ . We can write the EOMs in general as

$$\begin{aligned}\dot{\mathbf{P}}_1 &= \mathbf{H}_1 \times \mathbf{P}_1, \\ \dot{\mathbf{P}}_2 &= \mathbf{H}_2 \times \mathbf{P}_2.\end{aligned}\quad (62)$$

The Hamiltonians in the co-rotating frame are

$$\begin{aligned}\mathbf{H}_1 &= (+\omega_0 - \omega_c)\mathbf{B} + \mu(\mathbf{P}_1 - \mathbf{P}_2), \\ \mathbf{H}_2 &= (-\omega_0 - \omega_c)\mathbf{B} + \mu(\mathbf{P}_1 - \mathbf{P}_2).\end{aligned}\quad (63)$$

They have angles relative to the  $\mathbf{B}$ -direction of

$$\begin{aligned}\cos \theta_1 &= \frac{\omega_0 - \omega_c + \mu c_1 - \mu \alpha c_2}{\sqrt{(\omega_0 - \omega_c + \mu c_1 - \mu \alpha c_2)^2 + \mu^2(s_1^2 - \alpha s_2)^2}}, \\ \cos \theta_2 &= \frac{-\omega_0 - \omega_c + \mu c_1 - \mu \alpha c_2}{\sqrt{(-\omega_0 - \omega_c + \mu c_1 - \mu \alpha c_2)^2 + \mu^2(s_1^2 - \alpha s_2)^2}}.\end{aligned}\quad (64)$$

If we insert on the r.h.s. of each of these equations the expression for  $\omega_c$  from the corresponding lines in Eq. (58) we find that indeed  $\cos \theta_{1,2} = \cos \vartheta_{1,2}$ . Therefore, everything is self-consistent: The pure precession mode is a form of motion of both vectors where each is collinear with its Hamiltonian.

### C. Lepton-number conservation

With some mild restrictions as noted above, the pure precession mode is possible for almost any combination of  $\vartheta_1$  and  $\vartheta_2$ . In view of our application it is useful, however, to group this two-dimensional set of solutions into families of solutions that have a fixed “lepton number,” meaning solutions for which

$$D_{\parallel} = \cos \vartheta_1 - \alpha \cos \vartheta_2 \quad (65)$$

is a common fixed number. Each of these families includes the alignment case  $\vartheta_1 = \vartheta_2 \equiv \vartheta_0$  where  $D_{\parallel} = (1 - \alpha) \cos \vartheta_0$ . Therefore, we can write the condition of lepton-number conservation in the form

$$(1 - \alpha) \cos \vartheta_0 = \cos \vartheta_1 - \alpha \cos \vartheta_2. \quad (66)$$

In other words, once  $\alpha$  has been chosen, we can classify the solutions by the parameter  $\vartheta_0$  or equivalently by  $D_{\parallel}$ . All solutions with the same  $\vartheta_0$  form a family with the same lepton number and thus are adiabatically connected to the aligned case where  $\vartheta_1 = \vartheta_2 = \vartheta_0$ .

### D. Explicit solution

We are now in a position to find explicit solutions of the EOMs in the adiabatic limit where the two polarization vectors move in the pure precession mode. To this end we specify a value for  $\alpha$  and  $\vartheta_0$ , an angle that has the interpretation of twice the effective mixing angle. We can then use one of the tilt angles  $\vartheta_1$  or  $\vartheta_2$  as a parameter to characterize different solutions.

We know that the shorter anti-neutrino polarization vector  $\mathbf{P}_2$  for  $\mu \rightarrow 0$  will be anti-aligned with  $\mathbf{B}$  whereas  $\mathbf{P}_2$  will remain at some finite angle fixed by lepton-number conservation. Therefore,  $\vartheta_2$  is a more useful independent parameter. More specifically, we use

$$\eta \equiv \cos \vartheta_2 \quad (67)$$

as an independent variable that varies between  $\cos \vartheta_0 \geq \eta \geq -1$ . After eliminating  $\vartheta_1$  with the help of Eq. (66) it is trivial to find from Eq. (59) explicitly

$$\frac{\omega_c}{\omega_0} = \frac{\sqrt{1 - (c_0 - \alpha c_0 + \alpha \eta)^2} + \alpha \sqrt{1 - \eta^2}}{\sqrt{1 - (c_0 - \alpha c_0 + \alpha \eta)^2} - \alpha \sqrt{1 - \eta^2}}, \quad (68)$$

where  $c_0 \equiv \cos \vartheta_0 = \cos 2\theta_{\text{eff}}^\infty$ . Likewise, from Eq. (61) we find

$$\kappa = \frac{\sqrt{1 - (c_0 - \alpha c_0 + \alpha \eta)^2} - \alpha \sqrt{1 - \eta^2}}{2\sqrt{1 - \eta^2}\sqrt{1 - (c_0 - \alpha c_0 + \alpha \eta)^2}} \times \left[ (c_0 - \alpha c_0 + \alpha \eta)\sqrt{1 - \eta^2} - \eta\sqrt{1 - (c_0 - \alpha c_0 + \alpha \eta)^2} \right]. \quad (69)$$

While we cannot extract an explicit analytic result for  $\omega_c(\kappa)$ , we have an analytic form of this curve as  $\omega_c(\eta)$  and  $\kappa(\eta)$  in parametric form. Therefore, in contrast to Ref. [12] and in contrast to our box-spectrum example we do not rely on a numerical solution: All properties of the solution can be understood analytically.

In Fig. 11 we show  $\omega_c(\kappa)$  as a thin line for  $c_0 = \sqrt{0.75} = 0.866$ , corresponding to  $\sin 2\theta_{\text{eff}}^\infty = 0.5$ . This is equivalent to the thin line in the upper panel of Fig. 9, except that here we have two polarization vectors whereas there we had a double-box spectrum. The solutions are very similar. Using a smaller and smaller  $\sin 2\theta$ , corresponding to  $c_0$  approaching 1, the solution develops a sharper and sharper cusp as expected. We show the limiting curve for  $c_0 = 1$  or  $\sin 2\theta_{\text{eff}}^\infty = 0$  as a thick solid line.

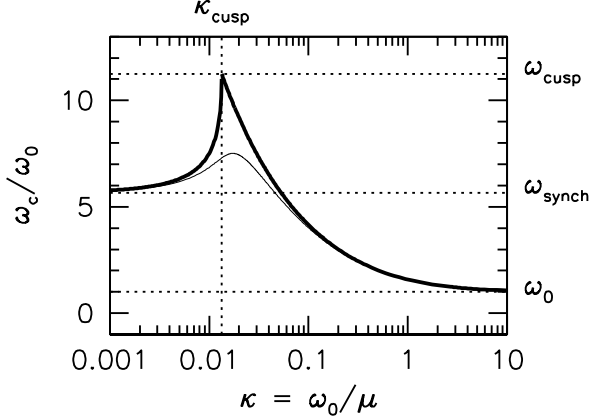


FIG. 11: Common precession frequency for our system of two polarization vectors with  $\alpha = 0.7$ , in full analogy to the double-box spectrum case of Fig. 9 (upper panel). The thick line is the limiting solution for  $\sin 2\theta_{\text{eff}}^\infty \rightarrow 0$ , equivalent to  $\cos \vartheta_0 \rightarrow 1$ , the thin line is for  $\sin 2\theta_{\text{eff}}^\infty = 0.5$ , corresponding to  $\cos \vartheta_0 = \sqrt{0.75} = 0.866$  as in Fig. 9.

### E. Cusp

The limiting case  $\cos \vartheta_0 \rightarrow 1$  involves a number of subtleties. In the strictly adiabatic limit this solution

corresponds to both polarization vectors being strictly aligned with  $\mathbf{B}$  or, in the neutrino language, to an exactly vanishing effective mixing angle. Starting with this initial condition, reducing the neutrino-neutrino interaction strength  $\mu$  could never lead to a deviation of the polarization vectors from this orientation just as in the absence of mixing there can be no flavor conversions.

We first study this limiting case by using  $c_0 = 1$  in Eqs. (68) and (69). The functions  $\omega_c(\eta)$  and  $\kappa(\eta)$  then give us only the large- $\kappa$  branch above the cusp. Specifically for  $\eta \rightarrow 1$  we find the familiar cusp values [11, 12]

$$\begin{aligned} \kappa_{\text{cusp}} &= \frac{(1 - \sqrt{\alpha})^2}{2} \\ &= 0.01334 \quad \text{for } \alpha = 0.7, \\ \frac{\omega_{\text{cusp}}}{\omega_0} &= \frac{1 + \sqrt{\alpha}}{1 - \sqrt{\alpha}} \\ &= 11.2444 \quad \text{for } \alpha = 0.7. \end{aligned} \quad (70)$$

Numerically these results are very similar to the double-box spectrum case, but not identical.

Let us begin with two polarization vectors in the pure precession mode with intermediate  $\mu$  and let us assume the conserved  $D_{\parallel}$  is such that in the alignment case they have  $c_0 = 1$ . If we now increase  $\mu$  adiabatically, alignment with each other and with  $\mathbf{B}$  is reached for  $\mu = \mu_{\text{cusp}}$  so that  $\vartheta_1 = \vartheta_2 = 0$ . As we increase  $\mu$  further until infinity, they cannot get more aligned. This is different for all cases with  $c_0 < 1$  where the angles keep monotonically decreasing with increasing  $\mu$  and reach alignment  $\vartheta_1 = \vartheta_2 = \vartheta_0$  only for infinite  $\mu$ .

### F. Sleeping-top regime

The range  $\mu_{\text{cusp}} < \mu < \infty$  in the limiting case has the interpretation of the “sleeping top regime” [12]. In the language of the gyroscopic flavor pendulum it corresponds to a spinning top that spins so fast that energy and angular momentum conservation prevent it from deviating from perfect vertical alignment if it was prepared in this state, seemingly defying the force of gravity. Therefore, we call this the sleeping-top range of  $\mu$  or  $\kappa$ .

We can study this regime using a somewhat different parametrization that allows us to take the limit of a small angle  $\vartheta_0$ . To this end we write  $\vartheta_2 = \xi \vartheta_0$  and thus express the tilt angles as multiples of  $\vartheta_0$ . In Eqs. (68) and (69) we thus substitute  $c_0 = \cos \vartheta_0$  and  $\eta = \cos \vartheta_2 = \cos(\xi \vartheta_0)$ . This is only a re-parametrization: Once more we can find, for any chosen value of  $\vartheta_0$ , the solution  $\omega_c(\kappa)$  in the parametric form  $\omega_c(\xi)$  and  $\kappa(\xi)$  with  $1 \leq \xi \leq \pi/\vartheta_0$ .

In the limit  $\vartheta_0 \rightarrow 0$  we find for the co-moving frequency

$$\frac{\omega_c}{\omega_0} = \frac{\sqrt{1 + \alpha(\xi^2 - 1)} + \alpha\xi}{\sqrt{1 + \alpha(\xi^2 - 1)} - \alpha\xi}. \quad (71)$$

This leading term in a  $\vartheta_0$  expansion does not depend on  $\vartheta_0$  and thus applies even for  $\vartheta_0 = 0$ . While in this case  $\vartheta_2 = \xi \vartheta_0 = 0$ , this result nevertheless depends on  $\xi$ .

For  $\xi = 1$  we reproduce the expected synchronization value of Eq. (60) whereas for  $\xi \rightarrow \infty$  we find  $\omega_{\text{cusp}}$  of Eq. (70). In other words, in the limit  $\vartheta_0 \rightarrow 0$  our new parametrization covers the sleeping-top branch, but not the region beyond the cusp.

One can take a similar representation for  $\kappa(\xi)$  and use only the leading term. This gives the limiting values  $\kappa(0) = 0$  and  $\kappa(\infty) = \kappa_{\text{cusp}}$  as expected.

Actually, Eq. (71) can be inverted to provide  $\xi(\omega_c)$  and the result can be inserted in the leading term of  $\kappa(\xi)$ , providing after some simplifications

$$\kappa = \frac{1}{\omega_c/\omega_0 + 1} - \frac{\alpha}{\omega_c/\omega_0 - 1}. \quad (72)$$

This function is well defined in the entire range  $\omega_{\text{cusp}} \leq \omega_c < \infty$ , i.e., once more we find both a physical and an unphysical branch of the solution. We can also invert this result and find for the physical branch

$$\frac{\omega_c}{\omega_0} = \frac{1 - \alpha - \sqrt{\alpha^2 - 2\alpha(1 + 2\kappa) + (1 - 2\kappa)^2}}{2\kappa}, \quad (73)$$

whereas the unphysical branch has a positive sign of the square root. This function has real values only for  $0 \leq \kappa \leq \kappa_{\text{cusp}}$  and indeed approaches the familiar limits  $\omega_{\text{synch}}$  and  $\omega_{\text{cusp}}$  at the two ends of the sleeping-top interval.

### G. Sum rules

The case of two polarization vectors studied in this section corresponds to the spectrum

$$P_\omega = \delta(\omega - \omega_0) + \alpha\delta(\omega + \omega_0). \quad (74)$$

The adiabatic solutions must obey the sum rules discussed earlier. For this two-line spectrum Eqs. (30) and (31) give

$$\begin{aligned} 1 &= \frac{1}{\sqrt{(\kappa - r\kappa + D_\parallel)^2 + D_\perp^2}} \\ &\quad - \frac{\alpha}{\sqrt{(-\kappa - r\kappa + D_\parallel)^2 + D_\perp^2}}, \\ r &= \frac{1}{\sqrt{(\kappa - r\kappa + D_\parallel)^2 + D_\perp^2}} \\ &\quad + \frac{\alpha}{\sqrt{(-\kappa - r\kappa + D_\parallel)^2 + D_\perp^2}}, \end{aligned} \quad (75)$$

where  $r \equiv \omega_c/\omega_0$ . For any two angles  $\vartheta_1$  and  $\vartheta_2$  we can calculate the corresponding  $D_\parallel$ ,  $D_\perp$ ,  $\omega_c$  and  $\kappa$  and show that the sum rules are actually fulfilled.

In the general case we used the sum rules to find solutions  $\omega_c(\kappa)$  and  $D_\perp(\kappa)$  and then find solutions for the individual polarization vectors which here would mean

to find  $\vartheta_1(\kappa)$  and  $\vartheta_2(\kappa)$ . In the two-polarization vector case we were able to proceed in the opposite way and find, for a given  $\vartheta_0$  (or a given  $D_\parallel$ ) the solutions  $\vartheta_1$ ,  $\omega_c$  and  $\kappa$  as a function of  $\vartheta_2$ . This was possible because for two polarization vectors lepton-number conservation uniquely fixes the angle  $\vartheta_1$  as a function of  $\vartheta_2$ .

### H. Spectral split?

For two polarization vectors a spectral split cannot occur because it would amount to the polarization vector  $\mathbf{P}_1$  breaking apart. The true final state consists of  $\mathbf{P}_2$  indeed anti-aligning with  $\mathbf{B}$  and  $\mathbf{P}_1$  retaining a non-zero transverse component. The  $\mathbf{P}_1$  final orientation is determined by lepton-number conservation. In the end it precesses freely around  $\mathbf{B}$  with frequency  $\omega_0$ . Indeed, we have found that in the end  $\omega_c^0 = \omega_0$ .

At the same time we have noted that in the pure precession mode the polarization vectors are aligned with their Hamiltonians which in the end seem to be (anti)parallel to  $\mathbf{B}$  because  $\mu = 0$ . Notice, however, that  $\mathbf{H}_1$  in Eq. (63) involves  $(\omega_0 - \omega_c)\mathbf{B}$  and if in the end  $\omega_c \rightarrow \omega_0$  the final length of  $\mathbf{H}_1$  approaches zero. In a limiting sense it always maintains a direction tilted against  $\mathbf{B}$  such that  $\mathbf{P}_1$  always remains aligned with  $\mathbf{H}_1$ .

Therefore, we here have a case where the perfectly adiabatic evolution leads to a final configuration where one of the polarization vectors is not (anti)aligned with  $\mathbf{B}$ .

For an arbitrary number of discrete polarization vectors an exact spectral split will usually not be possible because typically one of vectors would have to be broken apart to achieve a split. In this case the final  $\omega_c$  will be the  $\omega$  of the left-over polarization vector that can neither align nor anti-align with  $\mathbf{B}$  if lepton number is to be conserved. Therefore, we expect that in this situation the final adiabatic solution will be such that all polarization vectors (anti)align with  $\mathbf{B}$  except for this remaining one that sits on the fence and for which in the end  $(\omega - \omega_c) \rightarrow 0$ . In this way it remains aligned with its Hamiltonian alright. We have seen such a case in the fully adiabatic example in Fig. 8 where one mode ended up at  $P_{\omega_\parallel} = 0$ .

## VII. ADIABATICITY VIOLATION

### A. Sharpness of the spectral split

In practice,  $\mu(t)$  decreases with a finite speed. On the other hand, the  $\mathbf{P}_\omega$  with frequencies close to  $\omega_{\text{split}}$  precess very slowly at late times when  $\mu \rightarrow 0$ , so that adiabaticity is broken for those modes as discussed earlier. As a consequence, the spectral split is not infinitely sharp. There is a transition region of non-zero width. A quantitative estimate of the adiabaticity condition is given in our earlier paper [14].

The width of the transition region, i.e., the sharpness of the spectral split, is a common measure of the degree of adiabaticity also for the ordinary MSW effect where the split occurs at  $\omega = 0$ .

In order to quantify the meaning of “sharpness” we consider the example of neutrinos plus antineutrinos with a double-box spectrum with the average frequency  $\omega_0$  as in Sec. V and study the final neutrino spectrum. From Fig. 7 it is evident that the (anti)alignment of all polarization vectors with  $\mathbf{B}$  is almost perfect, even if adiabaticity is violated, except for the modes around the split. In Fig. 12 we show the final  $P_{\parallel}(\omega)$  and  $P_{\perp}(\omega)$  as a function of  $(\omega - \omega_{\text{split}})/\Delta\omega$ . Here,  $\Delta\omega$  is the variance or root-mean square width of the distribution  $P_{\perp}(\omega)$ . Of course, since  $P_{\omega}$  is conserved both distributions contain the same information, but  $P_{\perp}$  lends itself more directly to a straightforward definition of the width of the non-adiabatic range.

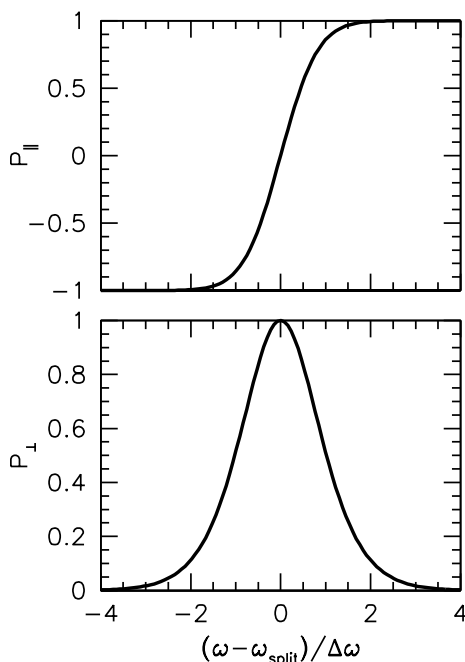


FIG. 12: Final spectra of  $P_{\parallel}(\omega)$  (upper panel) and  $P_{\perp}(\omega)$  (lower panel) for a double-box spectrum of neutrinos plus antineutrinos as in Sec. V. Here,  $\Delta\omega$  is the rms width of the distribution which depends on the time scale  $\tau$  for the exponential  $\mu(t)$  variation.

In this form, the shown functions appear to be universal for the assumed double-box spectrum as far as we can tell from a numerical exploration of parameters. In particular, these functions do not seem to depend on the assumed asymmetry parameter  $\alpha$ , not on the value of  $\omega_{\text{split}}$  and not on the mixing angle. They do not depend on the degree of adiabaticity, i.e., on the time scale  $\tau$  of the exponential  $\mu(t)$  variation, except through  $\Delta\omega$ . Varying  $\omega_0\tau$  over two decades between 10 and  $10^3$  we

find that

$$\Delta\omega \approx \omega_0 \frac{1}{(\omega_0\tau)^{3/4}} \quad (76)$$

is an excellent representation with an accuracy better than a few percent. (For  $\omega_0\tau = 100$  this implies  $\Delta\omega = 0.032\omega_0$ .) However, this relation is not exact: The dependence of  $\Delta\omega$  on  $\tau$  does not seem to be an exact power law. We give some explanations of these features in the following subsection.

### B. MSW effect vs. collective transformations

To shed more light on the dynamics of the split phenomenon we compare here the adiabaticity violation with its counterpart in the usual MSW case where the evolution is given by Eq. (4) with  $\mu = 0$  and where the EOMs for different frequencies  $\omega$  decouple.

Let us consider first the MSW case for the normal mass hierarchy. If the initial density is very large, much larger than the resonance density,  $\lambda \gg \lambda_{\text{res}}(\omega)$ , the initial effective mixing is strongly suppressed. The adiabatic evolution to small densities,  $\lambda \rightarrow 0$ , then leads to the well-known strong conversion with a final survival probability  $P = \sin^2\theta \approx 0$ . The neutrino polarization vector initially coincides with the Hamiltonian. Following the Hamiltonian completely flips the flavor. With increasing energy  $E$  (decreasing frequency  $\omega$ ) the degree of adiabaticity decreases and above a certain energy  $E_{\text{na}}$  the effects of adiabaticity violation increase exponentially.  $P$  increases and approaches 1. In the antineutrino channel for  $E \rightarrow \infty$  ( $\omega \rightarrow 0$ ) the mixing is strongly suppressed and the survival probability  $\bar{P} \approx 1$ . So, there is a continuity in the  $\omega$ -variable around  $\omega \sim 0$ , i.e., at the transition from neutrinos to antineutrinos.

The split frequency can be estimated using the Landau-Zener probability which describes well the survival probability for small mixing angles [22, 23]:  $P \approx P_{\text{LZ}} = e^{-A\omega}$ . Here  $A \equiv \pi\tau \sin^2 2\theta / (2 \cos 2\theta)$ , and  $\tau = \lambda/\dot{\lambda}$  is the scale height of the density change. From the condition  $P_{\text{LZ}} = 1/2$  we find

$$\omega_{\text{split}} = \frac{2 \ln 2}{\pi\tau} \frac{\cos 2\theta}{\sin^2 2\theta}. \quad (77)$$

For the width of the split region one finds  $\Delta\omega \sim \omega_{\text{split}}$  and  $\Delta\omega/\omega_{\text{split}}$  is a universal quantity that does not depend on the parameters of the problem. According to Eq. (77) the sharpness of the split is

$$\Delta\omega \propto \frac{1}{\tau} \quad (78)$$

which differs from the dependence in Eq. (76) for the collective transformation case.

We emphasize that here as well as in the collective transformation case the split phenomenon requires a specific initial condition: a small effective mixing angle.



For the MSW case in the normal mass hierarchy the split is in the neutrino channel and the flavor flips for  $\omega > \omega_{\text{split}}$ . For the inverted hierarchy the split is in the antineutrino channel and the modes with  $\omega < \omega_{\text{split}}$  flip.

With an increasing degree of adiabaticity (increasing  $\tau$ ) the split frequency shifts to smaller values, approaching  $\omega_{\text{split}} = 0$  which is realized in the ideally adiabatic case. Conversely, with a decreasing degree of adiabaticity both  $\omega_{\text{split}}$  and the width of the transition region increase. This differs from the collective transformation case where  $\omega_{\text{split}}$  does not shift and is determined solely by lepton-number conservation. In other words, the changes of  $\omega_c$  and  $D_\perp$  adjust themselves self-consistently in such a way that  $\omega_{\text{split}} = \text{const.}$  In the MSW case flavor lepton number is not conserved.

Let us consider the origin of the differences between these two cases. The Hamiltonian  $H_\omega = \mathbf{H}_\omega \cdot \boldsymbol{\sigma}$ , where  $\boldsymbol{\sigma}$  is the vector of Pauli matrices, has the diagonal and off-diagonal elements  $\pm H$  and  $\bar{H}$ , respectively,

$$2H = \mu D_\parallel - (\omega - \omega_c), \quad 2\bar{H} = \mu D_\perp. \quad (79)$$

The resonance condition,  $H = 0$ , can be written as

$$\omega = \mu_{\text{res}} D_\parallel + \omega_c(\mu_{\text{res}}). \quad (80)$$

The general form of the adiabaticity condition is  $\dot{\theta}_{\text{eff}} \ll \Delta H$ , where  $\theta_{\text{eff}}$  is the effective mixing angle and  $\Delta H$  the difference of eigenvalues. In the resonance region this condition takes on the form

$$\frac{\dot{H}}{4\bar{H}^2} \ll 1. \quad (81)$$

Using Eq. (79) we find explicitly

$$\frac{D_\parallel + \frac{d\omega_c}{d\mu}}{2\tau_\mu \mu_{\text{res}} D_\perp(\mu_{\text{res}})} \ll 1. \quad (82)$$

The transition to the usual MSW case is given by

$$\begin{aligned} \mu &\rightarrow \lambda, \\ (\omega - \omega_c) &\rightarrow \omega, \\ D_\parallel &\rightarrow L_\parallel = L \cos 2\theta, \\ D_\perp &\rightarrow L_\perp = L \sin 2\theta. \end{aligned} \quad (83)$$

A substantial difference is that in the MSW case both  $L_\parallel$  and  $L_\perp$  are constants and determined by the vacuum mixing angle. Moreover,  $\omega_c$  is absent. The resonance condition in the mass basis is:  $\omega = \lambda_{\text{res}} \cos 2\theta$ . The adiabaticity condition in the resonance becomes

$$\frac{1}{2\tau_\lambda \omega \sin^2 2\theta \cos 2\theta} \ll 1. \quad (84)$$

An essential difference of the collective case is that  $D_\perp$  is a dynamical variable and as such depends on  $\mu$ . Therefore the effective mixing angle changes not only due to the shrinking of the vector  $\mu\mathbf{D}$  in analogy to  $\lambda\mathbf{L}$  in the MSW

case, but also due to the rotation of  $\mathbf{D}$ . Consequently the width of the resonance layer, where  $2\theta_{\text{eff}}$  changes from  $45^\circ$  to  $135^\circ$ , and the adiabaticity condition essentially do not depend on the initial mixing angle. This explains the universality of the function that describes the spectral split.

The l.h.s. of the inequalities (82) and (84) are adiabatic parameters which, up to numerical coefficients, give the parameters in the exponents of the corresponding Landau-Zener probabilities. They determine how the sharpness of the spectral split depends on various parameters. Apparently Eq. (84) reproduces the result Eq. (78). In the collective case the dependence of  $\Delta\omega$  on  $\tau_\mu$  is more complicated due to the presence of  $\omega_c$  and  $D_\perp$  which depend on  $\mu$ . These functions are given in Fig. 9. Approximating these functions with power law functions in the resonance region and inserting them into Eq. (82) can provide an explicit expression for the shape of the washed-out spectral split.

### C. Initial alignment of polarization vectors

When we identified a sequence of static solutions with fixed lepton number and variable  $\mu$  as the adiabatic solution for a slow  $\mu(t)$  evolution, we assumed that initially  $\mu \rightarrow \infty$ . We assumed that initially all neutrinos are prepared in weak interaction eigenstates, corresponding to all  $\mathbf{P}_\omega$  being aligned in a direction that is tilted with the angle  $2\theta_{\text{eff}}^\infty$  relative to  $\mathbf{B}$ . This initial condition of perfect alignment corresponds to a pure precession solution only if  $\mu \rightarrow \infty$ .

In a realistic system  $\mu$  cannot be infinite. Therefore, if we begin with an initial condition of perfect alignment combined with a finite  $\mu$ , the system is initially not in a pure precession mode. Even if the subsequent  $\mu(t)$  evolution is infinitely slow, the polarization vectors will not be perfectly aligned with the Hamiltonians of the adiabatic solution.

In a linear system this situation would not spell a deviation from adiabaticity. Usually adiabaticity is taken to mean that the polarization vectors follow the Hamiltonians, but they need not be aligned with them. Rather, the precession cones would retain a non-zero but fixed opening angle.

Here the situation is different in that the  $\mathbf{P}_\omega$  define  $\mathbf{D}$  and thus affect the single-mode Hamiltonians  $\mathbf{H}_\omega$ . Therefore, these Hamiltonians must now themselves show fast motions when they are viewed from the co-rotating frame. Still, if the initial  $\mu$  is large (but finite), the deviation from a static solution is small and one expects that nonlinear effects appear only at second order in the small deviations of the polarization vectors from their adiabatic solutions. One would expect that the  $\mathbf{P}_\omega$  precess around the nearly static  $\mathbf{H}_\omega$  where the opening angle of the precession cone no longer vanishes. Notice that since  $\mathbf{D}$  depends on many modes the fast motion of the latter to some extent cancels in  $\mathbf{D}$  and therefore  $\mathbf{H}_\omega$ .

This behavior is borne out in numerical examples.

This numerical observation implies that the adiabatic solution is a stable fixed point of the system, i.e., a small perturbation does not lead to a run-away. Rather, the system always evolves close to the adiabatic solution and oscillates around it. The stability of the adiabatic solution is not automatically implied by its existence as a self-consistent solution of the EOMs. Since we do not have developed a formal criterion of stability, we do not know if there could be examples that would not be stable. Therefore, it is a numerical observation, not a proven fact, that the adiabatic solution is a good approximation to the exact solution for typical cases of realistic initial conditions.

#### D. Nutations

A system consisting of neutrinos and antineutrinos is similar to the neutrino-only case if one interprets the antineutrinos as negative-frequency modes, but it has a number of peculiar properties. One such a feature consists of the “wiggles” in the  $P_{\omega\parallel}$  evolution that we noted in the numerical solution of the EOMs shown in Fig. 8. The amplitude of these modulations becomes deeper if the effective mixing angle is smaller. To illustrate this point we show in Fig. 13 (top panel) the same example as in the upper-left panel of Fig. 8, now with a smaller mixing angle  $\sin 2\theta_{\text{eff}}^\infty = 10^{-3}$ .

Our general treatment shows that in the limit of a very slow  $\mu(t)$  variation and if initially  $\mu \rightarrow \infty$  all polarization vectors move in a co-rotating plane where the EOMs are solved by our adiabatic solution without wiggles. They are, therefore, a non-adiabatic feature and indeed disappear numerically if we use an unrealistically slow  $\mu(t)$  variation.

It has been shown that the EOMs of a system consisting of only two polarization vectors, one for neutrinos and one for anti-neutrinos as in Sec. VI, are equivalent to a gyroscopic pendulum in flavor space [11, 16]. Its general motion consists of a precession around  $\mathbf{B}$  and a nutation that causes the overall zenith-angle modulation. For very large neutrino-neutrino interactions (very small  $\kappa$ ), the pendulum is in the “sleeping top phase” [16] where its motion is a nearly pure precession. In the neutrino language this corresponds to the synchronized regime where all polarization vectors are strictly pinned to each other and precess around  $\mathbf{B}$  as a collective object. Once  $\kappa$  becomes larger than the “cusp value,” the gyroscope begins to wobble. In the neutrino language, this is the point where the polarization vectors begin to spread in the zenith-angle direction and are no longer strictly pinned to each other.

The nutations are excited because the flavor pendulum initially deviates only by the small angle  $2\theta_{\text{eff}}^\infty$  from the inverted vertical direction. Starting the pendular motion requires this small angle to grow under the influence of the external force, introducing a time scale that depends

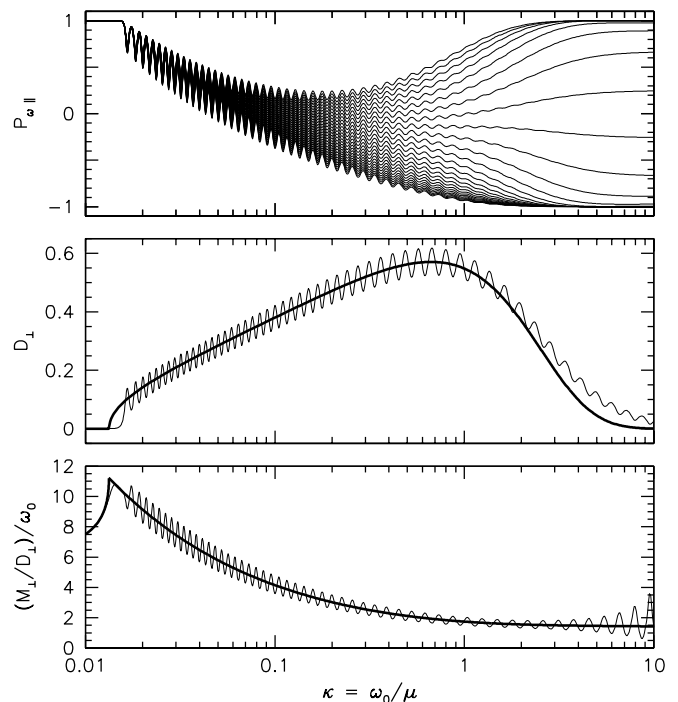


FIG. 13: Top:  $P_{\omega\parallel}(\mu)$  for 25 individual modes for the case of neutrinos plus antineutrinos. Same as upper left panel of Fig. 8, but now with a small mixing angle  $\sin 2\theta_{\text{eff}}^\infty = 10^{-3}$ . Middle:  $D_{\perp}$  calculated from the numerical solution compared with the adiabatic solution (thick line). Bottom:  $M_{\perp}/D_{\perp}$  in units of  $\omega_0$  calculated from the numerical solution compared with the adiabatic  $\omega_c$  (thick line).

logarithmically on  $2\theta_{\text{eff}}^\infty$ . If the  $\mu(t)$  variation is fast compared to this time scale, the pendulum cannot follow the adiabatic solution. This explains that the depth of the nutation amplitude becomes larger for a smaller  $2\theta_{\text{eff}}^\infty$ . The case of a vanishing  $2\theta_{\text{eff}}^\infty$  was the main example that we studied in Sec. V. While one can find a perfectly self-consistent static solution for this case, it is clear that the system cannot follow this solution: For a vanishing mixing angle the system will not move at all, i.e., the delay leading to nutations is infinite. Therefore, this example was an instructive limiting case, but cannot be realized as an adiabatically connected sequence of static solutions.

A remarkable feature of the nutations shown in Fig. 13 is that they are a collective effect of all modes. We cannot interpret the nutations as a simple precession of the individual  $\mathbf{P}_{\omega}$  around the static Hamiltonians. Rather, the nutations represent a motion of the entire system around the adiabatic solution. To illustrate this point we show in the middle panel of Fig. 13 the evolution of the numerical  $D_{\perp}$  in comparison with the corresponding adiabatic result. The true solution oscillates around the adiabatic solution with the nutation period. Likewise, the instantaneous precession frequency of the co-rotating plane, given by the quantity  $M_{\perp}/D_{\perp}$ , oscillates around the adiabatic result for  $\omega_c$  (bottom panel).

Once more we are numerically led to the conclusion

that the adiabatic solution represents a stable attractor of the nonlinear system. The true solution is a collective oscillation mode around this solution and thus plays the role of a perturbation. At the same time we stress that the individual  $\mathbf{P}_\omega$  evolve under the influence of their instantaneous Hamiltonians  $\mathbf{H}_\omega$  which are not identical with the ones of the adiabatic solution. The instantaneous Hamiltonians themselves nutate, although they nutate around the static Hamiltonians. We recall, however, that the instantaneous Hamiltonians always lie in a single plane, whereas this is not the case for the polarization vectors. Moreover, the motion of the instantaneous Hamiltonians is governed by the variation of the single vector  $\mathbf{D}$  so that they must move in lockstep with each other.

Another important feature of the nutations is that they are a transient phenomenon that dies out toward the end of the evolution when  $\mu \rightarrow 0$  as explained in the flavor pendulum picture [11, 16]. As a consequence, the spectral split remains unaffected. Even though all polarization vectors wildly nutate, they begin and end (anti)aligned with  $\mathbf{B}$  except for those modes near the split that anyway do not reach the final (anti)alignment. The modes sufficiently far from the split begin and end aligned with the static Hamiltonians, whereas for intermediate times they wildly nutate. The nutations have no apparent impact on the final flavor spectrum of the system.

### VIII. CONCLUSION

We have elaborated our previous theory [14] of spectral splits that occur as a consequence of the adiabatic evolution of a neutrino ensemble. We have clarified that the spectral-split phenomenon in itself is not an entirely new effect, but a very useful way of looking even at the usual MSW effect if we express its energy dependence in terms of the oscillation frequency  $\omega = \Delta m^2/2E$  and if we identify antineutrino modes with negative frequencies. However, in the case of collective transformations the effect has some distinctive features: the position of the split is fixed by the flavor lepton number of the system and does not depend on other parameters.

The main impact of collective neutrino-neutrino interactions is that the evolution is adiabatic not in the laboratory frame, but rather in a co-rotating frame that is defined by a plane in flavor space which is spanned by the mass direction  $\mathbf{B}$  and the vector  $\mathbf{D}$  which is the polarization vector of the overall flavor lepton number of the system. This frame defines a static solution of the EOMs that consists, in the laboratory frame, of a pure precession of all polarization vectors around  $\mathbf{B}$ . If the evolution in the co-rotating frame is adiabatic, we will have a sharp spectral split at the frequency  $\omega = 0$  in the co-rotating frame, corresponding to a frequency  $\omega_{\text{split}}$  in the laboratory frame where usually  $\omega_{\text{split}} \neq 0$ .

In order to take advantage of this picture we must find the co-rotating frame explicitly. This is achieved in terms

of two sum rules ( $\omega$ -integrals over the spectrum  $P_\omega$ ) that guarantee the self-consistency of the static solution, i.e., of the pure precession mode.

The main part of our paper is devoted to explicit analytical and numerical solutions of these equations (sum rules) for generic examples. The adiabatic solution is determined completely by two functions  $\omega_c(\mu)$  and  $D_\perp(\mu)$ . We study properties of these functions for several different neutrino spectra. For the neutrino-only box spectrum and non-zero initial effective mixing angle both functions decrease monotonically with  $\mu$ :  $\omega_c(\mu) \rightarrow \omega_{\text{split}}$  and  $D_\perp(\mu) \rightarrow 0$ .

In the presence of antineutrinos the behavior substantially changes: For small initial mixing angles the dependence  $\omega_c(\mu)$  has a cusp at a certain density  $\mu_{\text{cusp}}$ . The cusp corresponds to the border between the sleeping-top region and the beginning of bipolar transformations. Essentially the flavor evolution starts for densities below the cusp. Above the cusp,  $\omega_c(\mu)$  increases starting from the synchronization frequency. Below the cusp it decreases monotonically. With decreasing  $\mu$  we find that  $D_\perp(\mu)$  first increases, reaches a maximum at  $\mu \sim \omega_0$ , a typical frequency of the spectrum, and then decreases.

This type of behavior appears to be universal and shows up for completely different spectra. Very similar quantitative features appear for the continuous double-box spectrum and for the bi-chromatic spectrum. The latter case, by the gyroscopic flavor-pendulum analogy, allows one to understand a number of subtle features which also show up for continuous spectra.

The adiabatic solution is an approximate solution of the EOMs. There are several features which appear in the exact solution that are not described by the adiabatic solution. The violation of adiabaticity always takes place at late stages of evolution (at small  $\mu$ ) for modes with  $\omega$  close to  $\omega_{\text{split}}$ . This leads to a partial wash-out of the split so that the degree of adiabaticity determines the sharpness of the split. Numerically it appears that for a given spectrum the profile of the split is a universal function of the density gradient and does not seem to depend on other parameters. Measuring the width of the split region would allow one to determine the neutrino density gradient in the region  $\mu \sim \omega_0$ .

Nutations related to bipolar transitions represent another deviation from adiabaticity. The nutations occur around the adiabatic solution, or, in other words, the adiabatic solution appears as an average over nutations. Somewhat surprisingly, the nutations do not visibly influence the final result. They disappear as the neutrino density decreases and thus are only a transient phenomenon.

Our treatment leaves a number of interesting questions unresolved. While the self-consistency conditions determine the static solution, we have not realized under which circumstances such solutions actually exist, although we have not found a counter example.

The adiabatic solution is stable in typical numerical examples in that the true solution of the EOMs tracks this adiabatic solution. There could be situations where this

is not the case, leading to kinematical decoherence rather than a collective oscillation of the individual modes.

Even though several important aspects of this system are only numerically observed and not analytically proven, we believe that our adiabatic treatment of the EOMs nicely explains many of the intriguing features of this nonlinear system.

### Acknowledgments

This work was partly supported by the Deutsche Forschungsgemeinschaft under grant No. TR-27, by the

Cluster of Excellence “Origin and Structure of the Universe” (Munich and Garching), and by the European Union under the ILIAS project, contract No. RII3-CT-2004-506222. A.S. acknowledges support by the Alexander von Humboldt Foundation and hospitality by the Max-Planck-Institut für Physik during a visit where this work was begun.

- 
- [1] J. Pantaleone, “Neutrino oscillations at high densities,” *Phys. Lett. B* **287**, 128 (1992).
  - [2] S. Samuel, “Neutrino oscillations in dense neutrino gases,” *Phys. Rev. D* **48**, 1462 (1993).
  - [3] S. Samuel, “Bimodal coherence in dense selfinteracting neutrino gases,” *Phys. Rev. D* **53**, 5382 (1996) [hep-ph/9604341].
  - [4] Y. Z. Qian and G. M. Fuller, “Matter enhanced anti-neutrino flavor transformation and supernova nucleosynthesis,” *Phys. Rev. D* **52**, 656 (1995) [astro-ph/9502080].
  - [5] G. M. Fuller and Y. Z. Qian, “Simultaneous flavor transformation of neutrinos and antineutrinos with dominant potentials from neutrino neutrino forward scattering,” *Phys. Rev. D* **73**, 023004 (2006) [astro-ph/0505240].
  - [6] S. Pastor, G. G. Raffelt and D. V. Semikoz, “Physics of synchronized neutrino oscillations caused by self-interactions,” *Phys. Rev. D* **65**, 053011 (2002) [hep-ph/0109035].
  - [7] S. Pastor and G. Raffelt, “Flavor oscillations in the supernova hot bubble region: Nonlinear effects of neutrino background,” *Phys. Rev. Lett.* **89**, 191101 (2002) [astro-ph/0207281].
  - [8] H. Duan, G. M. Fuller and Y. Z. Qian, “Collective neutrino flavor transformation in supernovae,” *Phys. Rev. D* **74**, 123004 (2006) [astro-ph/0511275].
  - [9] H. Duan, G. M. Fuller, J. Carlson and Y. Z. Qian, “Simulation of coherent non-linear neutrino flavor transformation in the supernova environment. I: Correlated neutrino trajectories,” *Phys. Rev. D* **74**, 105014 (2006) [astro-ph/0606616].
  - [10] H. Duan, G. M. Fuller, J. Carlson and Y. Z. Qian, “Coherent development of neutrino flavor in the supernova environment,” *Phys. Rev. Lett.* **97**, 241101 (2006) [astro-ph/0608050].
  - [11] S. Hannestad, G. G. Raffelt, G. Sigl and Y. Y. Y. Wong, “Self-induced conversion in dense neutrino gases: Pendulum in flavour space,” *Phys. Rev. D* **74**, 105010 (2006) [astro-ph/0608695].
  - [12] H. Duan, G. M. Fuller, J. Carlson and Y. Z. Qian, “Analysis of collective neutrino flavor transformation in supernovae,” *Phys. Rev. D* **75**, 125005 (2007) [astro-ph/0703776].
  - [13] G. G. Raffelt and G. Sigl, “Self-induced decoherence in dense neutrino gases,” *Phys. Rev. D* **75**, 083002 (2007) [hep-ph/0701182].
  - [14] G. G. Raffelt and A. Y. Smirnov, “Self-induced spectral splits in supernova neutrino fluxes,” hep-ph/0705.1830.
  - [15] A. Esteban-Pretel, S. Pastor, R. Tomas, G. G. Raffelt and G. Sigl, “Decoherence in supernova neutrino transformations suppressed by deleptonization,” astro-ph/0706.2498.
  - [16] H. Duan, G. M. Fuller and Y. Z. Qian, “A simple picture for neutrino flavor transformation in supernovae,” astro-ph/0706.4293.
  - [17] H. Duan, G. M. Fuller, J. Carlson and Y. Q. Zhong, “Neutrino mass hierarchy and stepwise spectral swapping of supernova neutrino flavors,” astro-ph/0707.0290.
  - [18] G. L. Fogli, E. Lisi, A. Marrone and A. Mirizzi, “Collective neutrino flavor transitions in supernovae and the role of trajectory averaging,” hep-ph/0707.1998.
  - [19] A. S. Dighe and A. Y. Smirnov, “Identifying the neutrino mass spectrum from the neutrino burst from a supernova,” *Phys. Rev. D* **62**, 033007 (2000) [hep-ph/9907423].
  - [20] A. Dighe, “Supernova neutrinos: Production, propagation and oscillations,” *Nucl. Phys. Proc. Suppl.* **143**, 449 (2005) [hep-ph/0409268].
  - [21] G. Sigl and G. Raffelt, “General kinetic description of relativistic mixed neutrinos,” *Nucl. Phys. B* **406**, 423 (1993).
  - [22] W. C. Haxton, “Adiabatic conversion of solar neutrinos,” *Phys. Rev. Lett.* **57**, 1271 (1986).
  - [23] S. J. Parke, “Nonadiabatic level crossing in resonant neutrino oscillations,” *Phys. Rev. Lett.* **57**, 1275 (1986).